

B105076

REC'D FEB 8 1979
105076

AFML-TR-78-160
Volume I

MCIC-CAB DISTRIBUTION
Reviewer Date Used Rejected

ADB 034420

WARNING

Do not reference, loan or reproduce
this report without permission of
issuing agency.

COST EFFECTIVE REPAIR TECHNIQUES FOR TURBINE AIRFOILS

J. A. WEIN

W. R. YOUNG

GENERAL ELECTRIC COMPANY

AIRCRAFT ENGINE GROUP

CINCINNATI, OHIO 45215

NOVEMBER 1978

TECHNICAL REPORT AFML-TR-78-160, Volume I
Final Report 15 May 1978 — 15 July 1978

ber 1978 _____
_____ Wright-Patterson Air Force Base, Ohio 45433.

AIR FORCE MATERIALS LABORATORY
AIR FORCE AERONAUTICAL LABORATORIES
AIR FORCE SYSTEMS COMMAND
WRIGHT-PATTERSON AIR FORCE BASE, OHIO 45433



Private STINET

[Home](#) | [Collections](#)

[View Saved Searches](#) | [View Shopping Cart](#) | [View Orders](#)

Add to Shopping Cart

Other items on page 1 of your [search results](#): 1

[View XML](#)

Citation Format: Full Citation (1F)

Accession Number:

ADB034420

Citation Status:

Active

Citation Classification:

Unclassified

Fields and Groups:

010300 - Aircraft

130900 - Machinery and Tools

Corporate Author:

GENERAL ELECTRIC CO CINCINNATI OHIO AIRCRAFT ENGINE GROUP

Unclassified Title:

(U) Cost Effective Repair Techniques for Turbine Airfoils. Volume I.

Title Classification:

Unclassified

Descriptive Note:

Final technical rept. 15 May-15 Jul 78,

Personal Author(s):

Wein,J A

Young,W R

Report Date:

Nov 1978

Media Count:

82 Page(s)

Cost:

\$9.60

Contract Number:

F33615-76-C-5094

Report Number(s):

R78AEG430-VOL-1

AFML-TR-78-160-VOL-1

Monitor Acronym:

AFML

Monitor Series:

TR-78-160-VOL-1

Report Classification:

Unclassified

Descriptors:

(U) *AIRFOILS, *TURBINES, *REPAIR, COST EFFECTIVENESS, TURBINE COMPONENTS, MAINTENANCE MANAGEMENT, CRACKING(FRACTURING), NOZZLES, DIFFUSION BONDING, AIRCRAFT MAINTENANCE

Identifiers:

(U) *Turbine airfoils, LPN-AF-889-6

Identifier Classification:

Unclassified

Abstract:

(U) A program was conducted to establish cost effective repair procedures for conventionally cast turbine airfoils. Components selected for repair were the TF39 first and second stage turbine vanes and the TF39 first stage turbine blade as determined by a Phase I survey of ALC centers. Processes investigated include Activated Diffusion Healing (ADH) of turbine vanes and Activated Diffusion Bonding (ADB) of turbine blades by the mini-bond process. TF39 Stage 1 HPT vanes and TF39 Stage 2 HPT vanes were successfully processed through ADH repair by the Manufacturing Technology Laboratory (MTL), shipped to the General Electric Aviation Service Shop in Cincinnati for final processing and inspection, and are ready for Phase 3 engine testing. Pilot line processing of Stage 1 HPT blades provided an unsatisfactory yield due to a need for process control improvements. Action was taken to revise the Stage 1 HPT blade program to include use of MTL's new and improved minibonder and to try furnace ADB for additional attempts at bonding squealer tips and end caps to blade airfoils to obtain higher yields. (Author)

Abstract Classification:

Unclassified

Distribution Limitation(s):

01 - APPROVED FOR PUBLIC RELEASE

Source Serial:

F

Source Code:

403468

Document Location:

DTIC AND NTIS

IAC Assigned Accession Number:

MCIC-105076

Change Authority:

ST-A, AFWAL LTR, 6 OCT 81



[Privacy & Security Notice](#) | [Web Accessibility](#)

private-stinet@dtic.mil



NOTICES

When Government drawings, specifications, or other data are used for any purpose other than in connection with a definitely related Government procurement operation, the United States Government thereby incurs no responsibility nor any obligation whatsoever; and the fact that the Government may have formulated, furnished, or in any way supplied the said drawings, specifications, or other data is not to be regarded by implication or otherwise as in any manner licensing the holder or any other person or corporation, or conveying any rights or permission to manufacture, use, or sell any patented invention that may in any way be related thereto.

Copies of this report should not be returned unless return is required by security considerations, contractual obligations, or notice in a specific document.

This final report was submitted by General Electric Company, Aircraft Engine Group, Cincinnati, Ohio under Contract F33615-76-C-5094, Manufacturing Methods Project 889-6, "Cost Effective Repair Techniques for Turbine Airfoils." Mr. Fred R. Miller, AFML/LTM was the Project Monitor.

This technical report has been reviewed and is approved for publication.

Frederick R. Miller
FREDERICK R. MILLER
Project Manager

FOR THE DIRECTOR

H. A. Johnson
H. A. JOHNSON
Chief, Metals Branch
Manufacturing Technology Division

UNCLASSIFIED

SECURITY CLASSIFICATION OF THIS PAGE (When Data Entered)

REPORT DOCUMENTATION PAGE		READ INSTRUCTIONS BEFORE COMPLETING FORM
1. REPORT NUMBER AFML-TR-78-160 Vol I	2. GOVT ACCESSION NO.	3. RECIPIENT'S CATALOG NUMBER
4. TITLE (and Subtitle) COST EFFECTIVE REPAIR TECHNIQUES FOR TURBINE AIRFOILS	5. TYPE OF REPORT & PERIOD COVERED Technical Final 15 May 76 - 15 Jul 78	
	6. PERFORMING ORG. REPORT NUMBER R78AEG430	
7. AUTHOR(s) J. A. Wein W. R. Young	8. CONTRACT OR GRANT NUMBER(s) F33615-76-C-5094	
9. PERFORMING ORGANIZATION NAME AND ADDRESS General Electric Company Aircraft Engine Group (MTL) Cincinnati, Ohio 45215	10. PROGRAM ELEMENT, PROJECT, TASK AREA & WORK UNIT NUMBERS 889-6	
11. CONTROLLING OFFICE NAME AND ADDRESS Air Force Materials Laboratory (LTM) Wright-Patterson AF Base, Ohio 45433	12. REPORT DATE November 1978	
	13. NUMBER OF PAGES 70	
14. MONITORING AGENCY NAME & ADDRESS (if different from Controlling Office)	15. SECURITY CLASS. (of this report) UNCLASSIFIED	
	15a. DECLASSIFICATION/DOWNGRADING SCHEDULE	
16. DISTRIBUTION STATEMENT (of this Report) Approved for public release; distribution unlimited. <i>See Statement of Work</i>		
17. DISTRIBUTION STATEMENT (of this abstract entered in Block 20, if different from Report)		
18. SUPPLEMENTARY NOTES		
19. KEY WORDS (Continue on reverse side if necessary and identify by block number) Turbine blade and vane repair process Activated Diffusion Bonding Activated Diffusion Healing Fluoride Ion Cleaning Cost Reduction		
20. ABSTRACT (Continue on reverse side if necessary and identify by block number) A program was conducted to establish cost effective repair procedures for conventionally cast turbine airfoils. Components selected for repair were the TF39 first and second stage turbine vanes and the TF39 first stage turbine blade as determined by a Phase I survey of ALC centers. Processes investigated include Activated Diffusion Healing (ADH) of turbine vanes and Activated Diffusion Bonding (ADB) of turbine blades by the mini-bond process.		

DD FORM 1 JAN 73 1473

UNCLASSIFIED

SECURITY CLASSIFICATION OF THIS PAGE (When Data Entered)

TABLE OF CONTENTS

<u>Section</u>	<u>Page</u>
I INTRODUCTION	1
II IDENTIFICATION AND SELECTION OF REPAIRS OFFERING HIGHEST PAYOFF IN TOTAL ALC LIFE CYCLE MANAGEMENT	3
III ESTABLISHMENT OF REPAIR PROCESS FOR TURBINE NOZZLE AIRFOILS	10
1. TF39 Stage 1 HPT Nozzle Vane	10
2. TF39 Stage 2 HPT Nozzle Vane	27
IV ESTABLISHMENT OF REPAIR PROCESS FOR TURBINE BLADE AIRFOILS	61
1. TF39 Stage 1 HPT Blades	61

LIST OF ILLUSTRATIONS

FIGURE		PAGE
1	TF39 Stage I and II HPT Nozzle Vane and TF39 Stage I HPT Blade	5
2	Schematic Diagram of Mini-Bonder	6
3	Illustration of Fluoride Ion Cleaning Process	9
4	Service Induced Stress in TF39 Stage I HPT Nozzle Vane . . .	11
5	Configuration of Mechanical Property Test Specimens	14
6	Front and Side View of Tensile Specimen Showing Typical Failure Location	15
7	Tensile Properties of X-40 Parent Metal and ADH Joints at 1800°F	18
8	Stress Rupture Properties of X-40 Parent Metal and ADH Joints at 1800°F	19
9	Low Cycle Fatigue Properties of X-40 Parent Metal and ADH Joints at 1800°F	20
10	TF39 Stage HPT Vane at Incoming Inspection	22
11	Example of ADH Repair Alloy Application on TF39 Stage I HPT Vane	23
12	As ADH Repaired Condition of X-40 Engine Run TF39 Stage I HPT Vanes	24
13	Photomicrograph of ADB Repaired Cracks in X-40 Material . .	25
14	Finished TF39 Stage I HPT Vane Repaired by the ADH Process .	26
15	Appearance of Engine Run TF39 Rene' 80 Stage II HPT Vanes After Grit Blast Clean	29
16	Chemical Reactions During Cleaning in a Stable Fluoride Reducing Atmosphere	31
17	Equilibrium Constant K_p Versus Temperature for Fluoride Reduction Equation	32

LIST OF ILLUSTRATIONS

FIGURE		PAGE
18	HF Pressure Variation Versus Temperature for Equilibrium Fluoride Reduction Equation	33
19	Photomicrograph of Rene' 80 Airfoil Crack After Fluoride Ion Cleaning at 1800°F/One Hour	35
20	Graphic Illustration of Liquid Phase Sintering Before and After Casting	38
21	Rene' 80 Crack Repaired by Fluoride Ion Cleaning at 1800°F and ADH with D-15 Alloy	39
22	Rene' 80 1600°F Tensile Strength	44
23	Rene' 80 1700°F Stress Rupture Life	45
24	Rene' 80 1800°F Low Cycle Fatigue Life	46
25	SEM Analysis of Rene' 80 Crack Surface Before and After Fluoride Ion Clean	47
26	Rene' 80 Control Coupon for Effectiveness of F- Cleaning .	48
27	Stage II Vanes After 1000 Cycles Engine Test	49
28	Fluoride Ion Cleaned Vane After 1000 Cycles Engine Test .	50
29	Oxidation Characteristics of Rene' 80	52
30	Fluoride Ion Cleaned Vane, Chem Milled, Coated and Oxidized	53
31	Stage II HPT Vane Fluoride Ion Cleaned and Oxidized . . .	54
32	Stage II HPT Vane Fluoride Ion Cleaned, Grit Blasted, and Oxidized	55
33	TF39 Stage II HPT Vanes Positioned in Container for Fluoride Ion Clean Run	56
34	Typical Appearance of Fluoride Ion Cleaned and ADH Repaired TF39 Stage II HPT Vanes	58
35	Photomicrograph of Rene' 80 TF39 HP Vane ADH Repair After Complete Diffusion Cycle	59

LIST OF ILLUSTRATIONS

FIGURE		PAGE
36	View of Rene' 80 TF39 Stage II HPT Vane After Complete Processing	60
37	Stage I HPT Blade with Squealer Tip Cracks Extending Below Tip Cap	62
38	Mini-Bond Tip Replacement Concept on TF39/CF6-6 Stage I HPT Blade	63
39	Stress Rupture Tests of Rene' 80 and HS-188 ADB Joints at 2000°F	66
40	Inspection Fixture for Determination of ADB Joint Gap on Mini-Bonded Blade Tips	67
41	Bond Gap Measurement Locations	69
42	Blade to Cap Joint as Bonded Prior to a Heat Treat/ Diffusion Cycle	70
43	Blade to Cap Joint After a Heat Treat/Diffusion Cycle . .	70

LIST OF TABLES

TABLE		PAGE
1	Airfoil and ADB Alloys Used in Program	7
2	Pendulum Impact Specimens (X-40 Material)	16
3	Process Parameter Evaluation for Fluoride Ion Cleaning . . .	34
4	Pendulum Impact Specimens (Rene' 80 Material)	42

SECTION I

INTRODUCTION

Advanced turbine blades and vanes require the use of sophisticated air cooling techniques, costly nickel and cobalt base alloys, and extensive surface protective coatings. Because their operating environments cause various types of degeneration which ultimately lead to their removal and replacement, cost effectiveness of repair versus replacement must be considered in terms of overall life cycle management.

The purpose of the program initiated by Contract F33615-76-C-5094 was to establish cost effective repair techniques for conventionally cast turbine airfoils. The overall program objectives were:

- Select repair processes and airfoil types with generic application to ALC repair requirements.
- Transition advanced process to manufacturing technology.
- Verify repair procedures by pilot line production and component and/or engine test qualifications.
- Involve the Air Logistics Centers (ALC) at program inception with participation throughout to enable timely transition to the ALC's.
- Assess repair costs throughout the program to assure cost effectiveness when related to new part replacement cost.

To accomplish these objectives, General Electric conducted a four-phase manufacturing technology program within the Aircraft Engine Group. A team of contributors was assigned from Group Engineering and Group Manufacturing Divisions. By combining the disciplines of repair design, process development, manufacturing technology, and the Aviation Service Shops, the program was designed to insure rapid transition of repair technology to advanced turbine airfoils.

During Phase I, Repair Selection, a survey of ALC's was conducted. It resulted in the selection of TF39 high pressure turbine 1st and 2nd stage vanes and 1st stage blades as the generic repair components.

In Phase II, advanced processes were transitioned to manufacturing to establish the repair procedure. Each repair component was processed through a forty (40) piece pilot line to insure manufacturing process control and repeatability. The pilot line concept was used to provide an accurate assessment of the repair cost. Repair integrity was verified both by nondestructive inspection of appropriate coupon specimens and also by component metallographic examination.

Phase III included engine testing of components to qualify the repair procedure and Phase IV required documentation of the repair procedures by review and issuance of technical orders for repair of each component and analysis of the cost effectiveness of each repair.

Due to an unsatisfactory process yield obtained during the mini-bond repair of stage 1 HPT blades, it was decided to rerun the scale-up pilot line using improved materials and processes. Results of this additional effort for stage 1 blade repair will be discussed in a subsequent report (Volume II) along with engine test results of Phase III which had to be delayed due to limited availability of an engine test vehicle. Phase IV requirements for issuance of technical orders based on the pilot line repair procedures will follow examination and evaluation of the engine test hardware.

Cost Analysis for Cost Effective Repairs

Because of the provisioning policy utilized in acquisition of the TF39 engine system, a present day selling price for TF39 hardware cannot be accurately determined. However, for cost analysis purposes, a manufacturing price of comparable CF6 hardware will be considered on a relative scale of 100% for the most expensive component (i.e., new replacement HPT blade pair) so that the company's proprietary pricing policies are not exposed to the competitors. The cost effectiveness can then be determined as a function of new part replacement cost together with consideration of the comparison between presently accepted repair methods and those developed in this program. This phase of the program will be included in Volume II.

SECTION II

IDENTIFICATION AND SELECTION OF REPAIRS OFFERING HIGHEST PAYOFF IN TOTAL ALC LIFE CYCLE MANAGEMENT

Background

Turbine blades and vanes in current engines are subjected to the most hostile environment in the engine. As such, sophisticated airfoil designs and advanced materials have been developed to meet the stringent demands in the turbines of today's high performance engines. These turbine airfoils are usually investment castings containing internal cooling cavities. The materials used are high strength, high temperature resistant nickel or cobalt base superalloys. The parts are expensive -- often more than \$1000 each. Although long-life airfoils have evolved, damage still occurs -- cracking, foreign object damage, etc., which limit useful life. Because of the part costs it is obviously desirable to refurbish the complex turbine blades/vanes.

Survey Results

A survey was conducted to establish the highest generic repair payoff potential in turbine vanes/blades. The criteria used included:

- Incidence of damage - Scrapped or damaged turbine airfoils at the ALC centers were reviewed and types of damage noted.
- Replacement cost of component - ALC replacement costs and current new parts costs were reviewed. ALC's were requested to provide additional data on parts considered applicable to generic repair.
- Life of repaired part -- As was discussed with ALC's, repaired part life should equal new part life based on CF6 engine experience.
- Repair costs -- ALC's indicated the need to keep repair costs below 60% of new replacement parts cost. Repaired vanes are estimated to be between 30-50% of the cost of a new replacement part.
- Generic applicability -- The TF39 turbine airfoils selected for the program will be applicable to generic repair of turbine airfoils manufactured from nickel or cobalt base materials.
- Urgency to ALC's -- The ALC's verified the need for advanced turbine vane repair techniques and the urgency of new technology to increase repair capability and yield. At present, significant quantities of turbine airfoils are scrapped as "non-repairable".

This survey was coordinated with AFML, the Air Logistics Centers at San Antonio and Oklahoma City, GE Field Services representatives and program representatives from the GE Evendale plant.

Preselected repair priorities established by General Electric were reviewed with the ALC's at San Antonio, Texas and Oklahoma City, Oklahoma and met with their concurrence. Based on ALC coordination and inputs, it was established that the hardware suitable for development of generic repairs would be TF39 stage 1 high pressure turbine blades and stages 1 and 2 high pressure turbine vanes, shown in Figure 1.

The previously identified criteria formed the basis for ranking of cost effective repairs. Two specific types were identified as providing the highest potential payoff for repair applications.

- blade tip replacement
- cleaning and healing cracks in airfoils

Blade Tip Replacement by Mini-Bonding

General Electric recently developed a new manufacturing process called Mini-Bonding. Mini-Bonding is a superalloy joining process whereby jet engine components can be fabricated (for either initial fabrication or for repair) both rapidly and inexpensively. The process involves a combination of Activated Diffusion Bonding and localized vacuum induction heating. The bonding load, i.e., the force necessary to produce intimate contact of the bond surfaces during bonding, is provided by a movable piston, which applies atmospheric pressure over the cross-sectional area of the piston (see Figure 2). Patents have been applied for on the Mini-Bonder and are now pending.

Mini-Bonding differs from furnace Activated Diffusion Bonding primarily in the following ways: (1) Furnace ADB heats the entire component, including bulky fixturing -- Mini-Bonding, via high frequency induction, heats only the joint region, (2) Furnace bonding is both slow and expensive (i.e., several hours per run and a minimum \$125,000 facility investment) -- Mini-Bonding is rapid and less expensive (3-5 minutes per blade with a \$50,000 facility cost) and, (3) Furnace ADB uses dead weight loading to produce joint pressure -- Mini-Bonding uses atmospheric pressure over the cross-sectional area of a movable piston. With Mini-Bonding's ability to apply a greater joint load, joint efficiencies approaching parent metal are achievable.

The Mini-Bonding facility used for the initial efforts consisted of: (1) a high frequency (450 KHz), 5 KW power supply, (2) a high vacuum pumping system, (3) a small vacuum chamber which houses the coil, the blade fixture and the movable load piston and, (4) a radiation sensing head (to read temperature).

Fluoride Ion Cleaning and ADB Crack Healing

Contemporary jet engines predominantly use nickel base superalloys as turbine airfoils -- alloys such as Rene' 77, Rene' 80 with nominal chemistry shown in Table 1. After engine exposure the surfaces of these complicated airfoils are covered with stable surface oxides which severely inhibit repair operations such as stripping, re-welding, re-brazing, etc. The need for crack-penetrating cleaning method for nickel superalloys was clear.

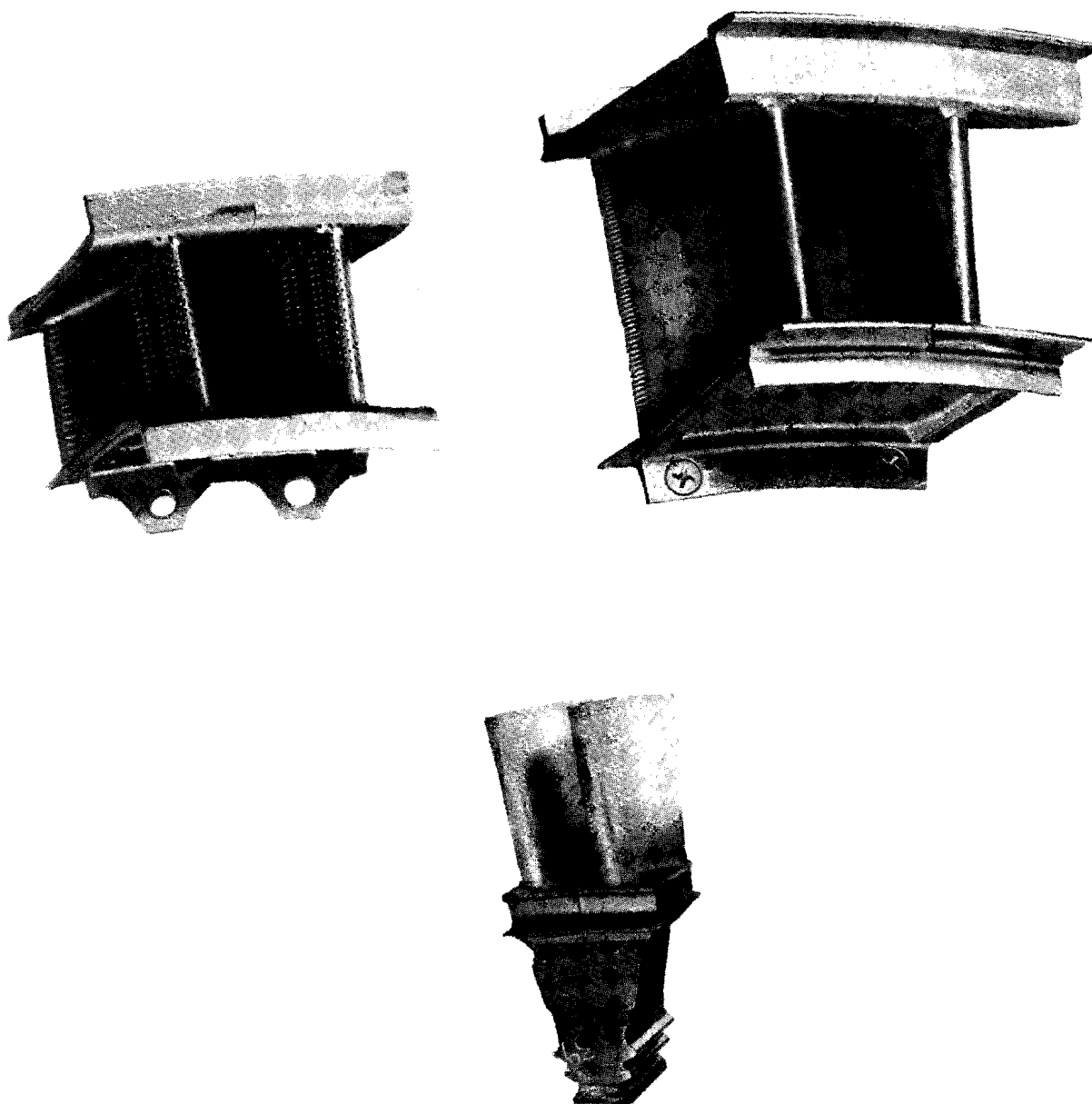


Figure 1. TF39 Stage 1 and 2 HPT Nozzle Vane
TF39 Stage 1 HPT Blade

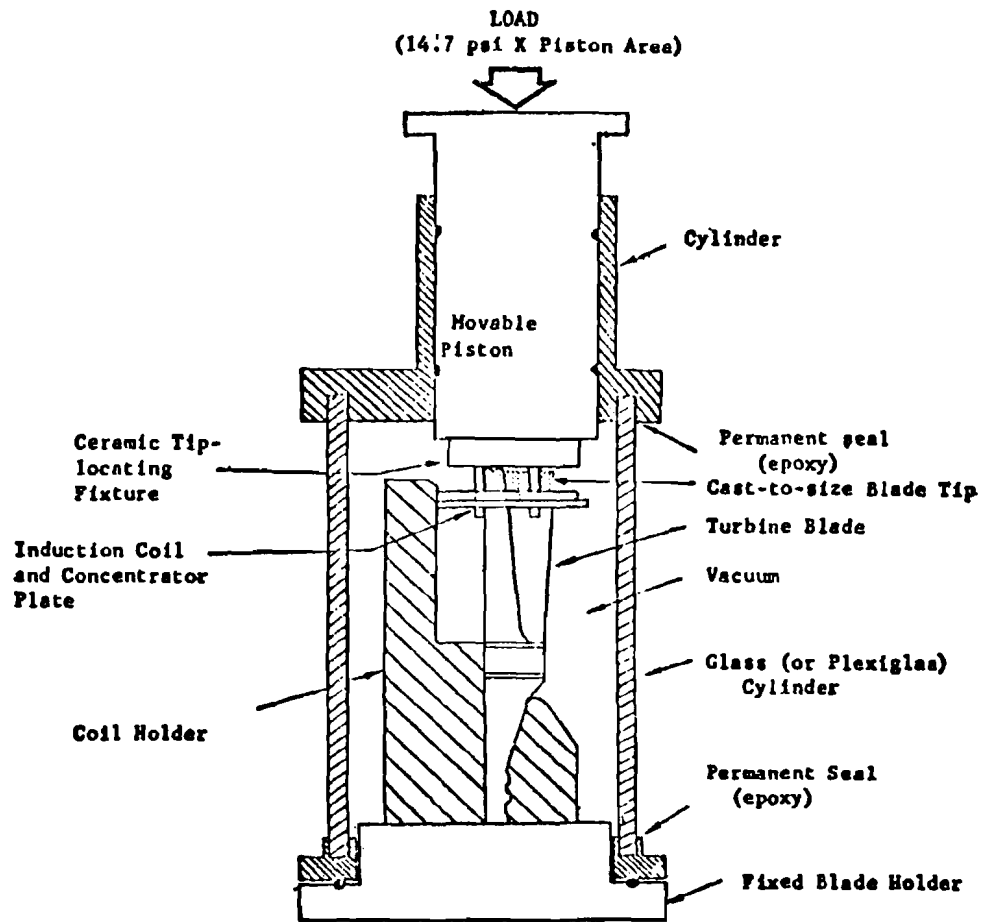


Figure 2. Schematic of the Mini-Bonder Showing the Chamber, the Coil, the Blade (& Tip) and Movable Piston

2

[illegible]

General Electric overcame this cleaning problem through development and use of a gaseous cleaning medium, containing the active fluoride ion, which reduces and removes stable Al/Ti containing oxides from turbine airfoil crack surfaces. The process, being gaseous, removes oxides from surfaces inside, outside, within cooling holes, and from cracks. Oxide removal has been repeatedly confirmed by metallography, Scanning Electron Microscope (SEM) analysis of crack surfaces before and after cleaning, and perhaps most dramatically, by fluid flow of brazing alloy over the cleaned surfaces and into the cleaned cracks. The fluoride ion process uses simple heat treat equipment -- a hydrogen atmosphere retort in an air furnace -- almost identical to the production diffusion coating systems used in most overhaul and repair shops in this country.

General Electric developed the fluoride ion cleaning process and demonstrated its capabilities and limitations over the past three years. Initially, the cleaning technology reported by ONERA of France⁽¹⁾ was combined with the GE Codep coating experience; both of which use the fluoride ion in a gaseous atmosphere. A conceptual illustration of the process is shown in Figure 3. The gaseous atmosphere containing the fluoride ion flowing over and through the oxidized cracks in turbine airfoils reduce the stable metal oxides. At the same time metal fluoride vapors are formed and are vented from the retort with the water vapor formed by the combination of hydrogen and the liberated oxygen.

Activated Diffusion Bonding (ADB) is a joining process for superalloys, developed by General Electric, which involves the marriage of conventional brazing to solid state diffusion bonding technology to achieve high joint strengths. The process involves joining nickel-base superalloy components with a specially designed bonding alloy (GE alloy D-15) that completely melts at an elevated temperature, (e.g., 2200°F for Rene' 80) below the incipient melting point of the alloy being joined. The bonding alloy is basically a high strength superalloy modified by boron and/or silicon to achieve a lowered melting range. Although considerable diffusion occurs during the bonding cycle, subsequent heat treatment effects homogenization of the chemistries of the bonding alloy and base metal. For filling of wide cracks or build up of worn base material, metallic powder of base metal composition is combined as a mixture with the ADB (D-15) alloy to develop joint properties comparable to the superalloy base material.

The ADB alloys used for this program are also shown in Table 1. ADB has been used for high strength joining in nearly all of the currently-used turbine airfoil and sheet superalloy materials including Rene' 100, Rene' 80, Rene' 120, Rene' 125, HS188, Rene' 77, Hastelloy X and others. ADB alloys are used for high strength brazing in nearly every contemporary GE engine including the TF39, TF34 and F101.

The actual utilization of a specific bonding alloy applied over eroded or cracked airfoil surfaces with subsequent diffusion and heat treatment is now referred to as Activated Diffusion Healing (ADH).

1. Genieys, E. "Brazing in Reducing Fluoride - Containing Atmospheres", 1st International Brazing & Soldering Conference, London, November 1972.

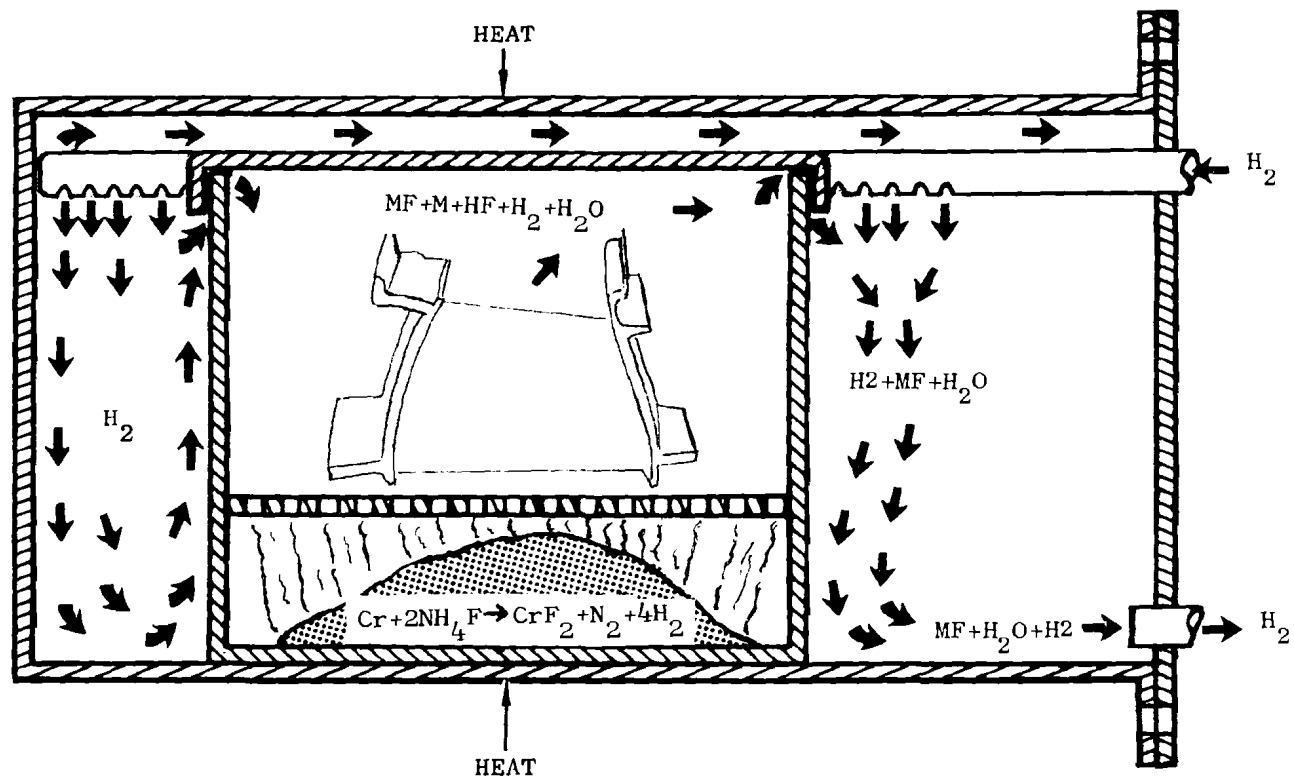


Figure 3. Illustration of Fluoride-Ion Cleaning Process

SECTION III

ESTABLISHMENT OF REPAIR PROCESS FOR TURBINE NOZZLE AIRFOILS

1. TF39 STAGE 1 HPT NOZZLE VANE

The TF39 stage 1 turbine nozzle vane is a cast X-40 cobalt base alloy which is both convectively and film cooled by compressor discharge air. Typical service induced distress is shown in Figure 4. TO repair allowances restrict weld repair to inner/outer platform and flange/seal surfaces. Commercial repair of comparable CF6-6 hardware incorporates extensive welding for refurbishment on platforms, certain airfoil, and flange surfaces. However, leading edge thermal cracks represented a condition which was not repairable because of excessive cost. This particular condition represented over 90% of non-repairable parts. It was apparent that if a procedure could be developed for leading edge crack repair, it would also be applicable to nearly all other distressed areas. The process which was selected to accomplish this particular repair and which appeared to provide the cost effectiveness needed to make it successful, utilized technology developed from activated diffusion bonding (ADB). As applied to crack repair in turbine nozzle airfoil and platform surface restoration, this new process was referred to as activated diffusion healing (ADH).

A cost analysis was made to aid in selection of the specific procedure and sequence to be used to accomplish the ADH repair. Cost comparison was made between:

- 1) Identification and repair of individual cracks versus application of quantities of ADH alloy to specific areas because of observed repetitive distress (zone alloying).
- 2) ADH filling of cooling holes with subsequent EDM of new holes versus hole dimensional maintenance during ADH repair.
- 3) Identification of individual part dimensional discrepancies versus a standardized, repetitive build-up.

For this piece of hardware, it was found that the latter case in each instance was more cost effective. For example, the identification and repair of individual cracks with subsequent remachining of the filled holes was more costly than zone alloying of the airfoil and platform with manual installation of quartz rod pins for dimensional hole maintenance. Based on this analysis and the typical distressed areas observed in the stage 1 vane component, a preliminary repair sequence was identified and is shown below:

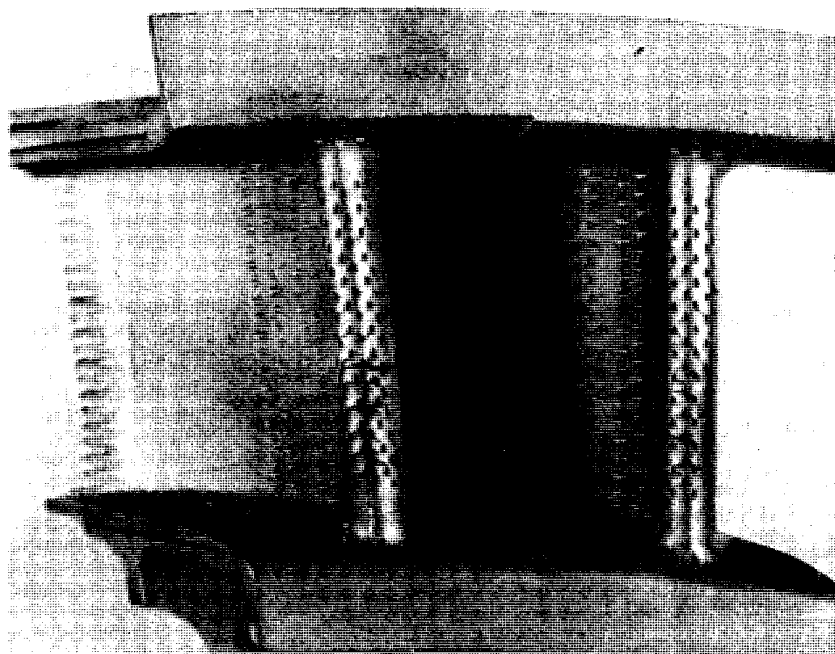
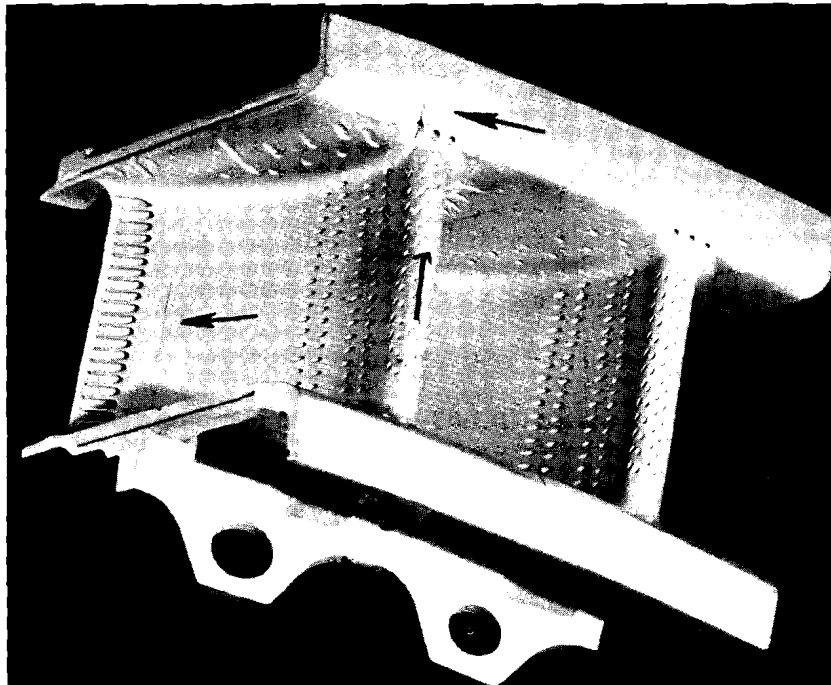


Figure 4. Service Induced Stress in TF39 Stg 1
HPT Nozzle Vanes

- a) Incoming clean - 120 grit Al_2O_3 at 100 psi max.
- b) Identification, bushing removal, and incoming inspection.
- c) Remove inserts.
- d) Hot forming to straighten and restore dimensions.
- e) Dimensional inspection.
- f) Strip Codep coating and residual braze alloy.
- g) Remove shallow cracks (0.003-0.005-inch deep) on vane airfoil surface by dry abrasive blast.
- h) Fluorescent penetrant inspect and map defects.
- i) Vapor degrease.
- j) Stress relieve and clean at 2150-2200°F/2 hrs. in hydrogen (-60°F Dewpoint).
- k) Install quartz pins in cooling air holes to prevent hole plugging during ADH, as required.
- l) ADH repair cracks and build-up dimensions as determined by prior inspections.
- m) Remove quartz pins in 50% hydrofluoric acid, inhibited.
- n) Visual inspect and blend repair areas.
- o) Dimensional inspection.
- p) Fluorescent penetrant inspect.
- q) Inspect vane holes for plugging and EDM open as required.
- r) Polish nozzle airflow surfaces.
- s) Codep coat.
- t) Install nozzle cooling air inserts.
- u) Machine nozzle build-up areas to restore dimensional requirements.
- v) Dimensional and fluorescent penetrant inspection.

- w) Water flow and airflow test.
- x) Install bushing in mounting flange.
- y) Final dimensional inspection.

This procedure incorporates the same processes used in weld repair of commercial CF6 vanes with the exception of the hydrogen clean and ADH alloy application and healing cycle.

Substantiation for this process sequence now becomes a function of evaluation of the selected ADH alloy for mechanical properties and microstructure and determination of cleaning effects from the hydrogen stress relieve cycle.

ADH Alloy Selection

Two powder blended alloy mixtures were screened for use as an ADH filler material for the Stage 1 HPT vane repair. A proprietary 50% D-15/50% X-40 mixture was compared with an 80% H-33/20% X-40 mixture. Joint strength properties were comparable. However, the improved flow characteristics of the H-33/X-40 mixture together with the manufacturing advantage of being able to perform the ADH repair in vacuum or hydrogen were deciding factors in selecting this alloy for use over the D-15/X-40 mixture. Additionally it was found that a post repair diffusion heat treatment was unnecessary.

The two alloys were compared at room temperature in tensile shear using a 2T overlap specimen with a .250" gage width. The specimens were made by machining a standard tensile strip specimen (see Figure 5) from .060" cast X-40 sheet and abrasively cutting the specimen in half. A flowthrough shear joint was made by application of each alloy as a slurry to the overlap side and brazing at 2200°F for 30 minutes. Three specimens of each alloy were tested using a 3000#/min. load rate with the average results summarized below:

ROOM TEMPERATURE TENSILE SHEAR STRENGTH			
Parent Metal	ADH Alloy	UTS (ksi)	Cross Sectional Area
X-40	X-40/D-15	41.7	0.031
X-40	X-40/H-33	47.7	0.031

In all cases the failure occurred in the X-40 base metal at the edge of the overlap fillet radius and a typical failure is shown in Figure 6.

"Nil-Strength"* of Joints in X-40 Material

The over-temperature capabilities of the two alloys were evaluated for bonding X-40 material: the X-40/D-15 mixture and X-40/H-33 mixture. The 50% X-40/50% D-15 joint sheared at 2300°F while the 80% H-33/20% X-40 joint sheared at 2250°F. As a comparison, X-40 base metal fails in the same test at approximately 2425°F.

*Nil-Strength - The temperature at which a bonded joint is incapable of sustaining a small, steady-state load of 125 psi.

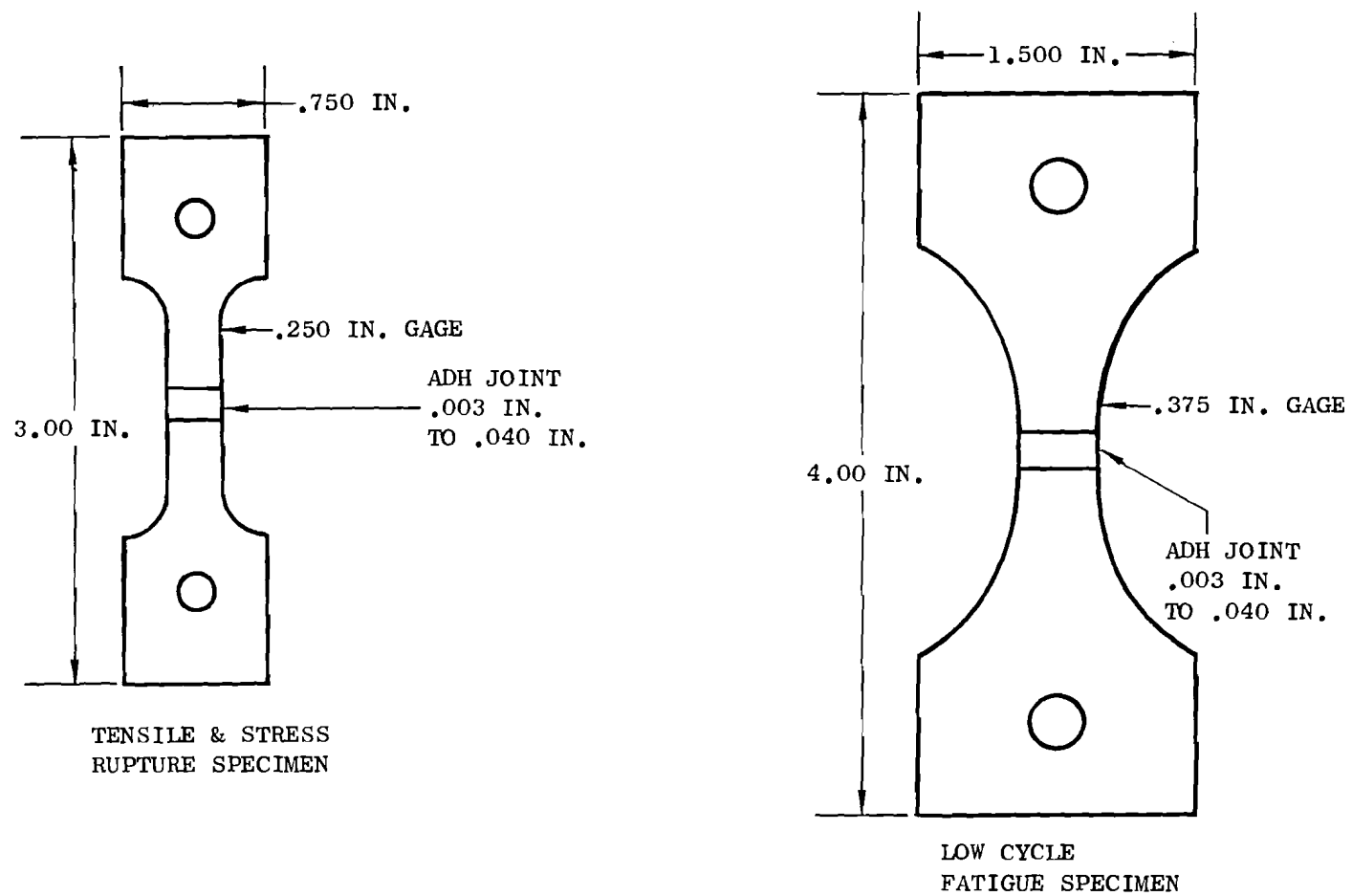
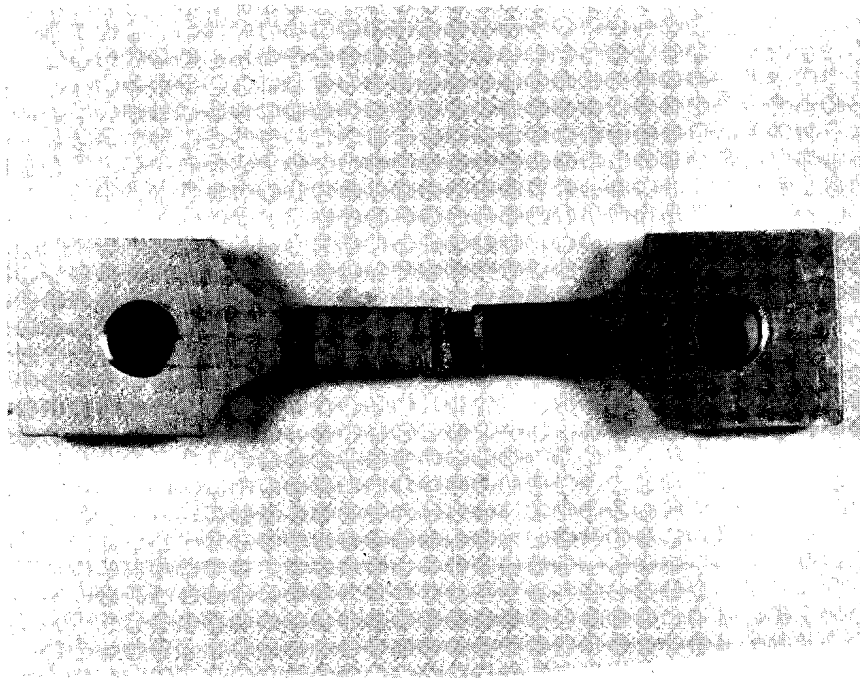
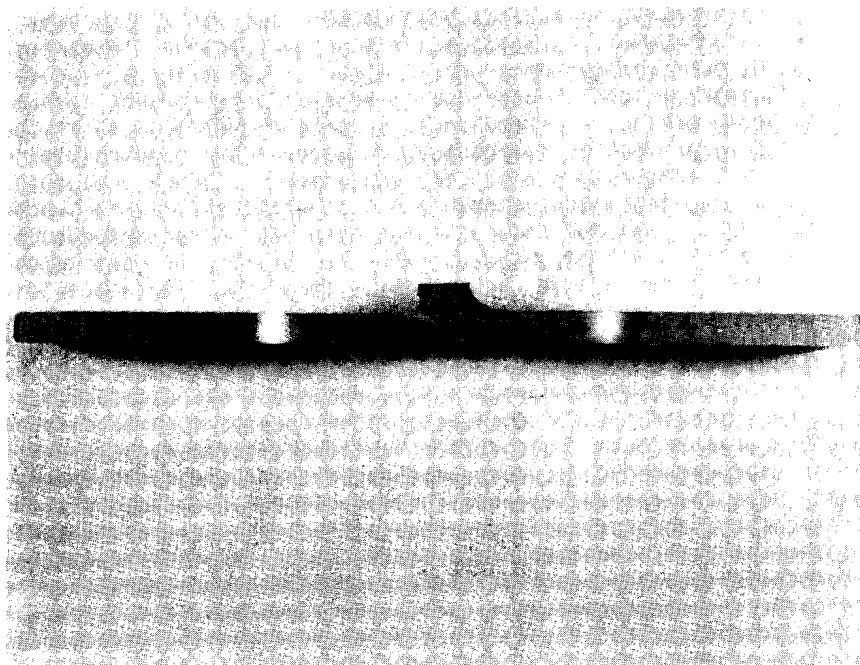


Figure 5. Configuration of Mechanical Property Test Specimens



1.5X



1.5X

Figure 6. Front and Side View of Tensile Shear Specimen
Showing Typical Failure Location

Pendulum Impact

Testing was conducted on specimens machined from 0.060" cast X-40 sheet. The impact specimens were manufactured by joining two strips 1.5" long by 0.500" wide with a butt joint. Gap variation was controlled from 0.003" to 0.040". A Charpy Impact tester was utilized with the impact directly on the joint. The data is presented in Table 2 and reflects the room temperature toughness of the bonding alloy along with representative X-40 parent metal results.

TABLE 2

PENDULUM IMPACT PARENT METAL SPECIMENS			
	Width at Impact	Material Thickness	Failure Load
X-40 Flat Sheet	0.473	0.064	1.67 ft-lb
	0.450	0.066	2.35 ft-lb
	0.495	0.065	2.46 ft-lb
	0.430	0.065	1.14 ft-lb
	0.474	0.069	2.63 ft-lb

PENDULUM IMPACT SPECIMENS (X-40 Material - H-33/X-40 Bonding Alloy 80/20 Mix-Flat Sheet)				
Gap of Bond Joint	Width at Joint	Thickness of Joint	Failure Location	Failure Load Ft-Lb
0.003 inch gap	0.445	0.064	P	1.71
	0.469	0.064	P	1.37
	0.442	0.064	J	1.27
	0.461	0.064	J	1.72
	0.451	0.057	P	2.80
	0.451	0.057	P	3.49
0.010 inch gap	0.440	0.064	J	1.12
	0.453	0.064	P	2.05
	0.429	0.056	J	1.54
	0.457	0.056	J	3.17
	0.453	0.063	J	3.21
	0.443	0.063	P	2.75
0.020 inch gap	0.437	0.063	J	3.83
	0.469	0.063	P	2.68
	0.445	0.059	J	2.10
	0.457	0.059	J	1.39
	0.461	0.064	P	1.91
	0.432	0.064	P	4.75
0.040 inch gap	0.447	0.062	J	1.71
	0.452	0.062	P	2.04
	0.443	0.059	J	2.14
	0.446	0.059	J	2.39
	0.455	0.061	J	2.22
	0.473	0.061	J	1.65

P = Parent Metal Failure

J = Bond Joint Failure

Mechanical Properties of X-40 Joints

Elevated temperature tensile, stress rupture and low cycle fatigue tests were conducted to determine the effect of the cleaning process on parent metal properties. Similar testing was conducted to determine the joint efficiency of the ADH joints with gaps of 0.003, 0.010, 0.020, and 0.040 inch.

A sketch of the test specimens is shown in Figure 5. The X-40 alloy was in the form of 0.060-inch thick cast sheet. Gaps for the ADH specimens were achieved by placing appropriate shims between the edges of two blanks and tack welding them in place at the outer edge of the specimen blanks. These shims were part of the scrap when the gage section was machined.

The effect of the cleaning process was determined by testing of the parent metal in three conditions:

- Control condition was fully heat treated and codep coated.
- Oxidized and strip condition was used to simulate the engine repair condition.
- Oxidized + strip + hydrogen clean condition was used to isolate the effect on properties of the hydrogen cleaning process.

The oxidation exposure of 100 hours at 1800°F in static air was done on Codep coated specimens. The strip cycle is the standard Codep stripping cycle. Hydrogen cleaning was done at 1800°F for 1 hour at a dewpoint of -60°F, although this parameter was later increased to 2 hours at 2150-2200°F during scale-up of the process.

The effect of joint gap filled with ADH alloy was determined on fully heat treated and Codep coated test specimens. The X-40 ADH cycle was 2200°F for 30 minutes in vacuum followed by the Codep cycle of 1925°F for 4 hours. The ADH alloy was 80% H-33/20% X-40.

Test Results

The 1800°F tensile results are shown in Figure 7. Equivalent ultimate and 0.2% yield strength values are shown for all parent metal and ADH joints tested.

The 1800°F stress rupture results plotted in Figure 8 show a reduction in life for the ADH repair. The commercial weld repair which uses L-605 alloy filler is also plotted on the graph. It has improved load carrying ability over the ADH alloy up to 1000 hours life. However, at longer times the ADH repair will be superior.

The 1800°F load controlled low cycle fatigue tests were run in an axial-axial tension mode using an A ratio of 0.95 and a cycle rate of 20CPM.

The results are shown in Figure 9. The effect of gap width is not significant. However, a joint reduces the cyclic load carrying ability by 40%. The hydrogen cleaning also is shown to cause a reduction in life for the limited tests conducted. This effect was not evident in either stress rupture or tensile testing.

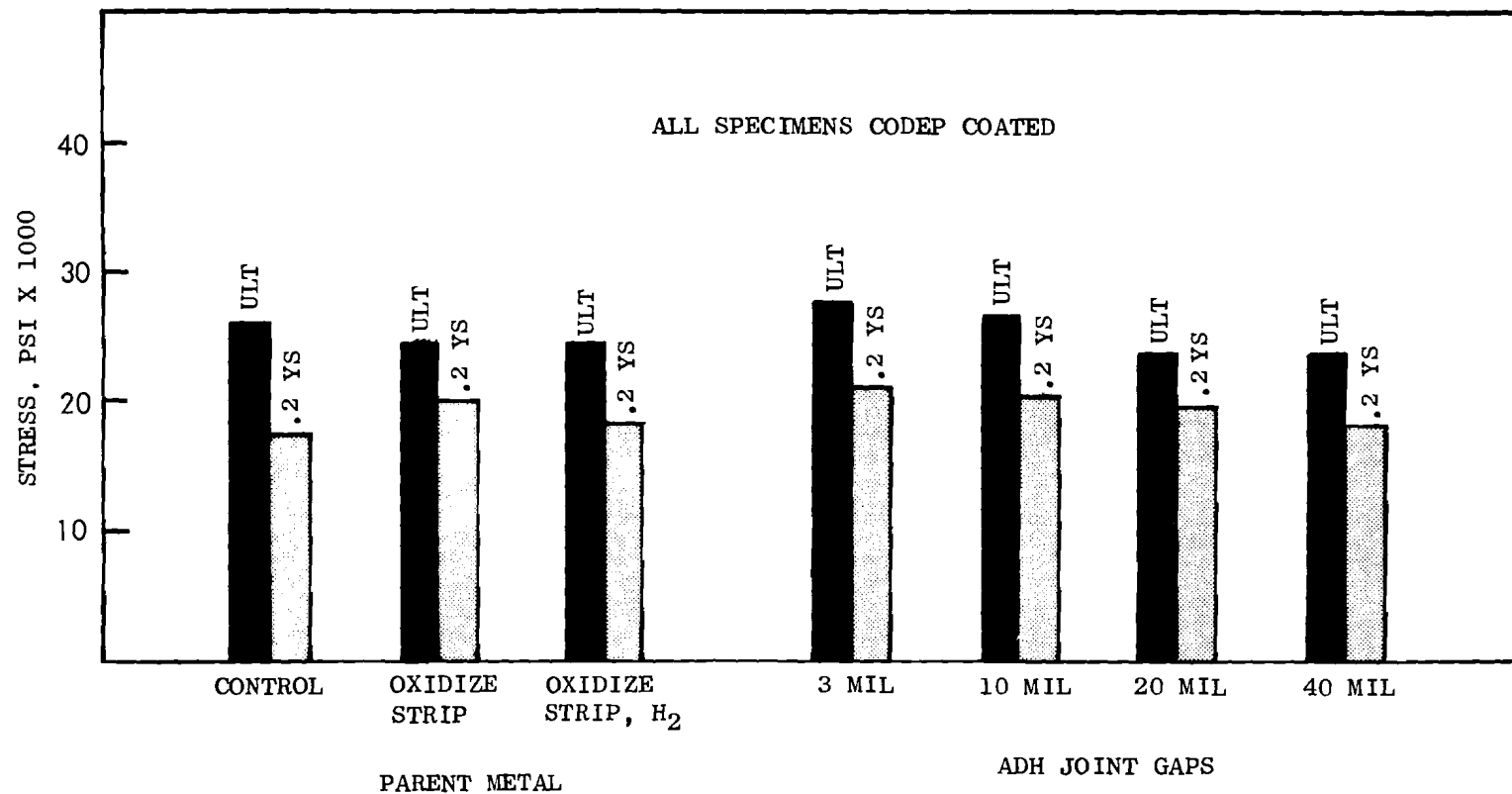


Figure 7. Tensile Properties of X-40 Parent Metal and Activated Diffusion Healed (ADH) Joints at 1800°F

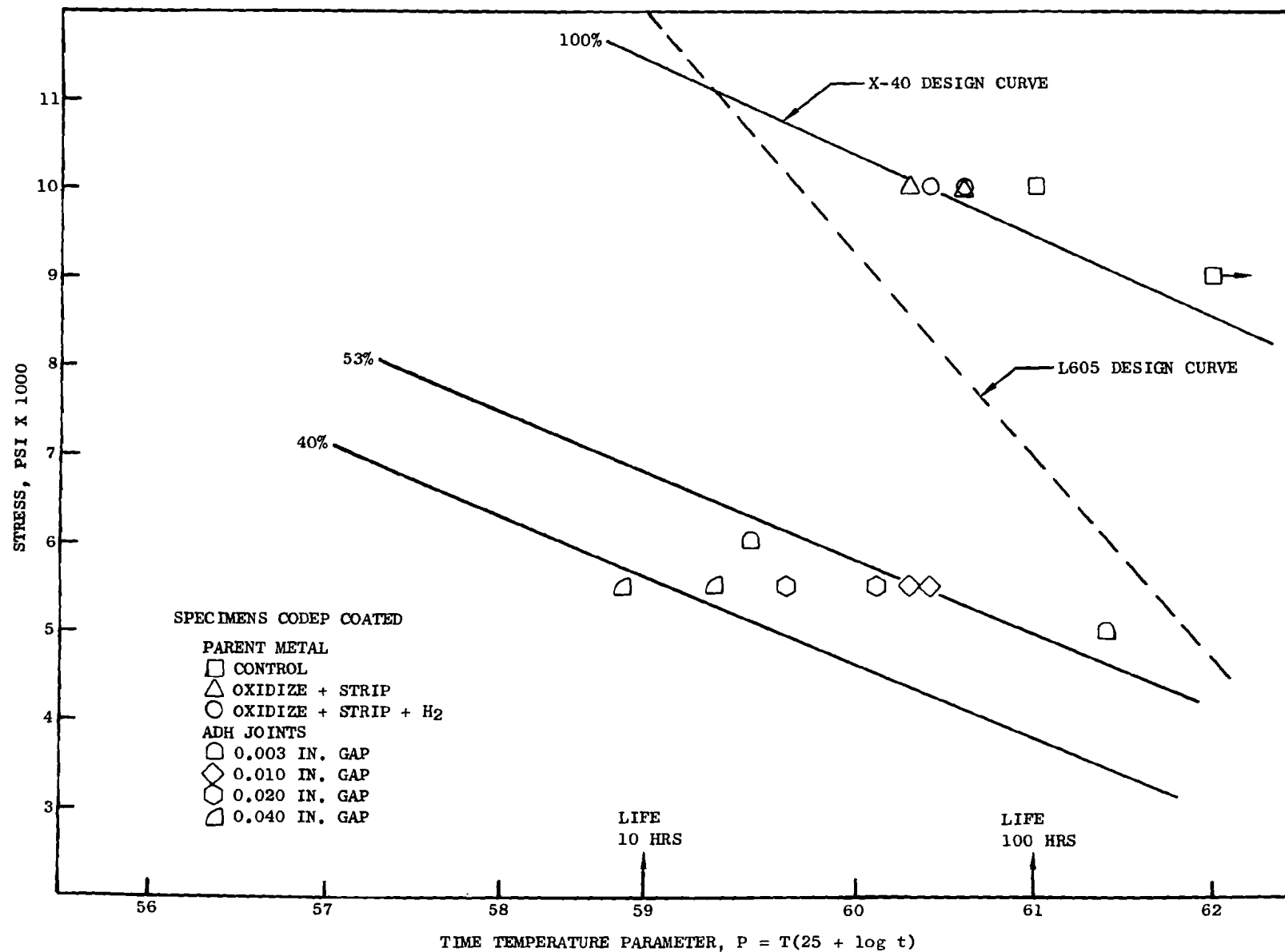


Figure 8. Stress Rupture Properties of X-40 Parent Metal and Activated Diffusion Healed (ADH) Joints at 1800°F

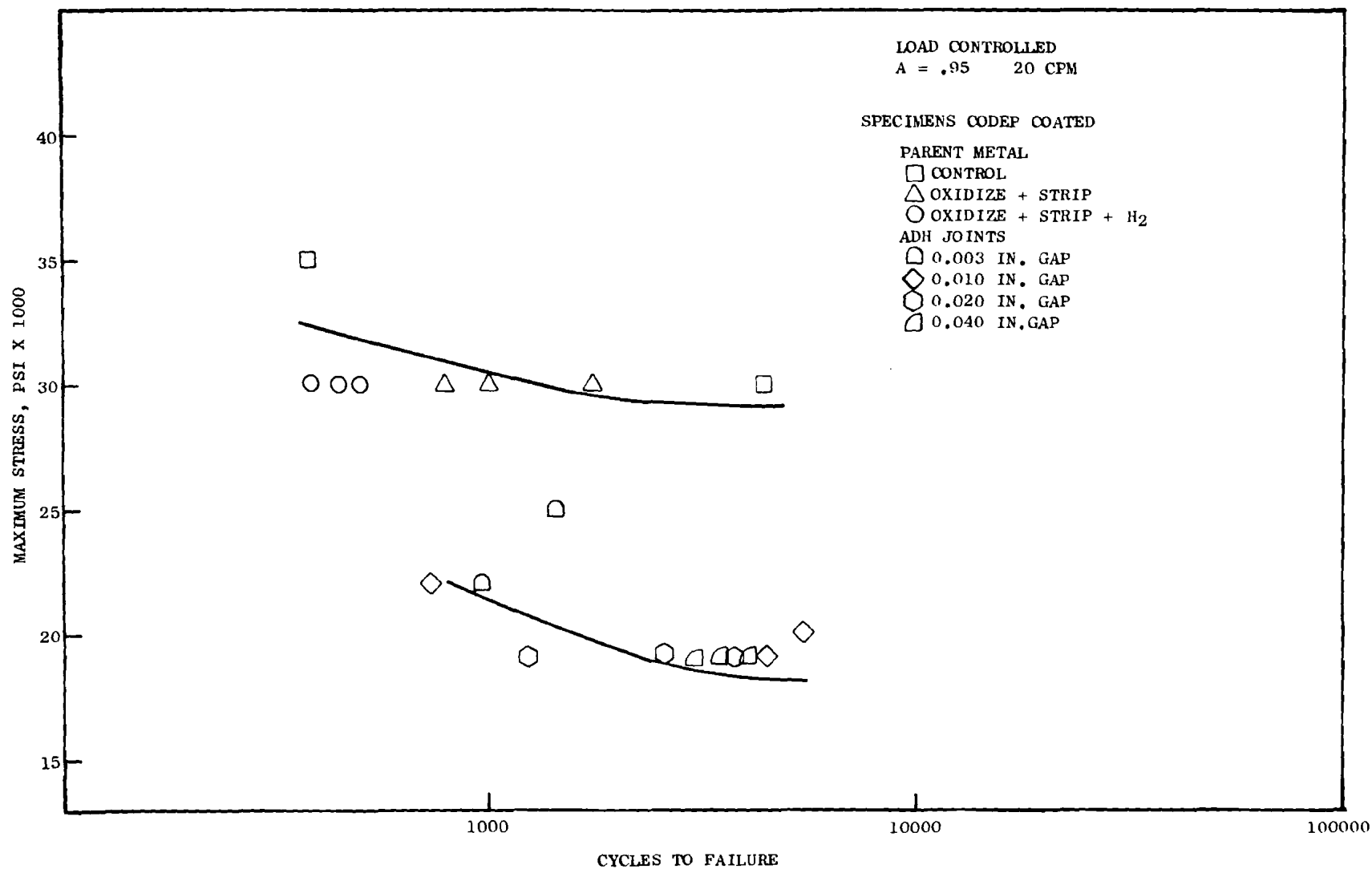


Figure 9. Low Cycle Fatigue Properties of X-40 Parent Metal and Activated Diffusion Healed (ADH) Joints at 1800° F

In summary, these tests indicate ADH joint strengths will experience reductions from parent metal properties, however there is no effect of joint gap on tensile and LCF properties. This will permit extensive ADH repairs since the 0.040 inch gap was selected to represent the worst condition for allowable repair.

Scale-Up of Repair Process

Scale-up of the repair process for the TF39 stage 1 HPT vane was accomplished through use of a 40 piece pilot line operation. This method best serves the interest of determining process cost and identifies potential problem areas associated with new processes.

Scale-up of hydrogen cleaning the X-40 stage 1 HPT vanes prior to ADH repair disclosed some inconsistency in results when attempting to perform the hydrogen clean cycle at 1800°F for 1 hour. Based on studies performed at Aerobrazo, Woodlawn, Ohio, it was verified that stress relieving and hydrogen cleaning the X-40 at 2150-2200°F for 2 hours in a hydrogen atmosphere with a dewpoint of -60°F or better produced satisfactory results and this has been incorporated into our current processing procedures. Since the higher cleaning temperature being used is still equal to or lower than the 2200°F used for subsequent ADH crack repair, only limited testing was conducted on specimens hydrogen-cleaned at 2150°F 2 hours. There was no strength reduction in tensile, fatigue, or rupture properties.

Because of the extensive cracking and severe leading edge distress, typified in Figure 4 & 10, it was found to be more cost effective to use a zone alloying concept with maintenance of cooling hole dimensions by installing quartz rod pins. This method is shown in Figures 11 and 12.

Some concern arose as to selection of the H-33/X-40 alloy when benching to remove excess alloy indicated that the mixture was much softer than the parent metal X-40. To prevent a possible program setback, two additional alloys were applied to five vanes to be engine tested along with those originally planned for engine run. These alloys consisted of a 40% X-40/60% H-33 mixture and a 50% D-15/50% X-40 mixture. These five additional vanes were processed along with the original 40 piece pilot lot. Representative microstructures are shown in Figure 13. Mechanical property data is not available on the D-15/X-40 mixture at this time.

All excess repair alloy was either hand-blended from the airfoil surfaces or machined from the flange build-up areas. The repaired vanes met all dimensional and airflow requirements imposed on new parts. FPI inspection requirements met were the same as those required for parts repaired by the current TO weld repair method. Figure 14 shows a typical TF39 stage 1 HPT vane processed through the complete pilot line.

The process yield for the forty piece pilot line lot (plus 5 additional vanes) was 100 percent. It is anticipated that in repair shops greater than 95% yields can be obtained with one repair cycle. Additional repair cycles would increase final yield to near 99%.

The repaired vanes have been submitted for TF39 engine test and results are expected early in 1979, with preliminary inspection in late 1978.

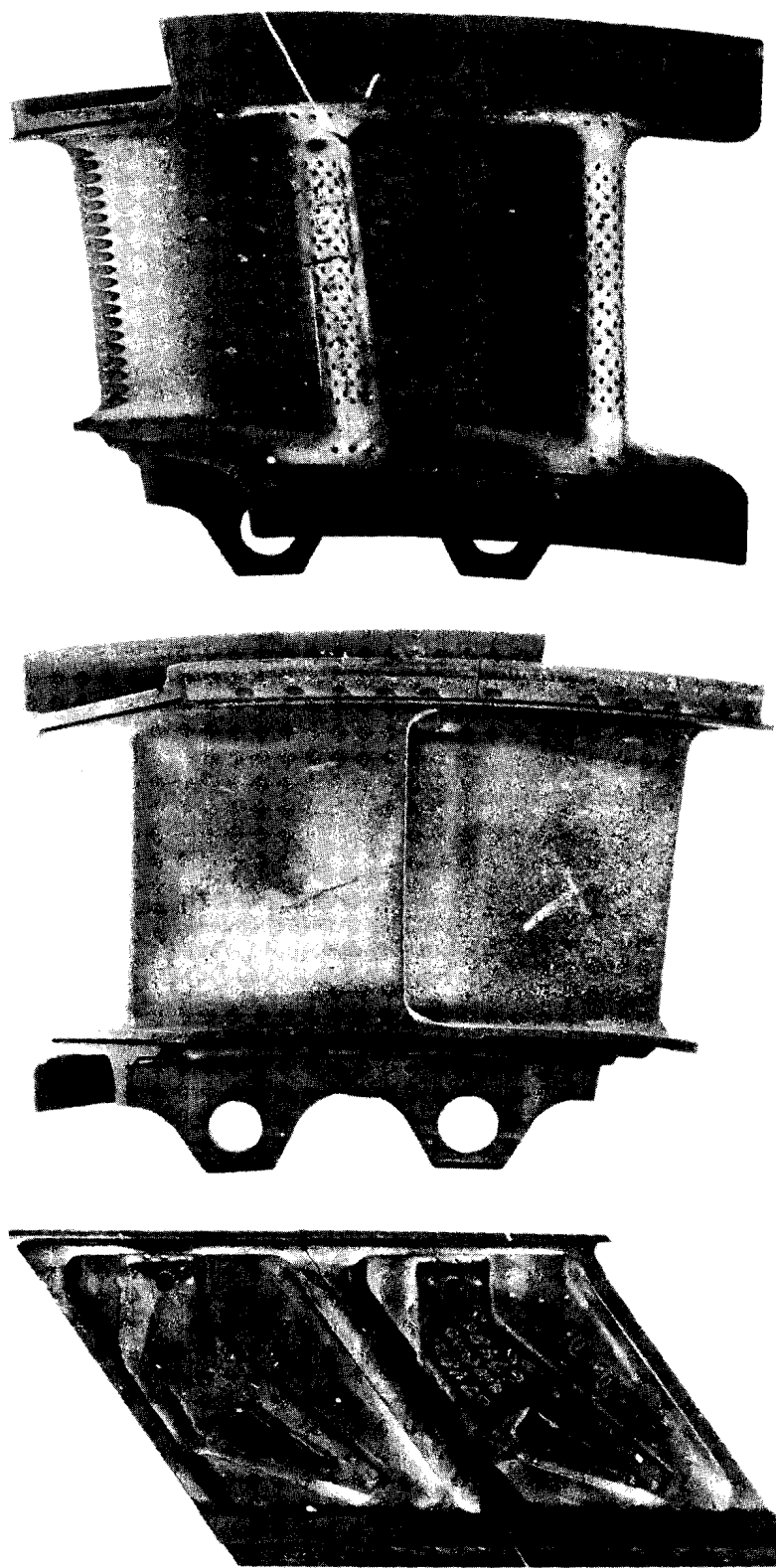


Figure 10. TF39 Stage 1 HPT Vane at Incoming Inspection

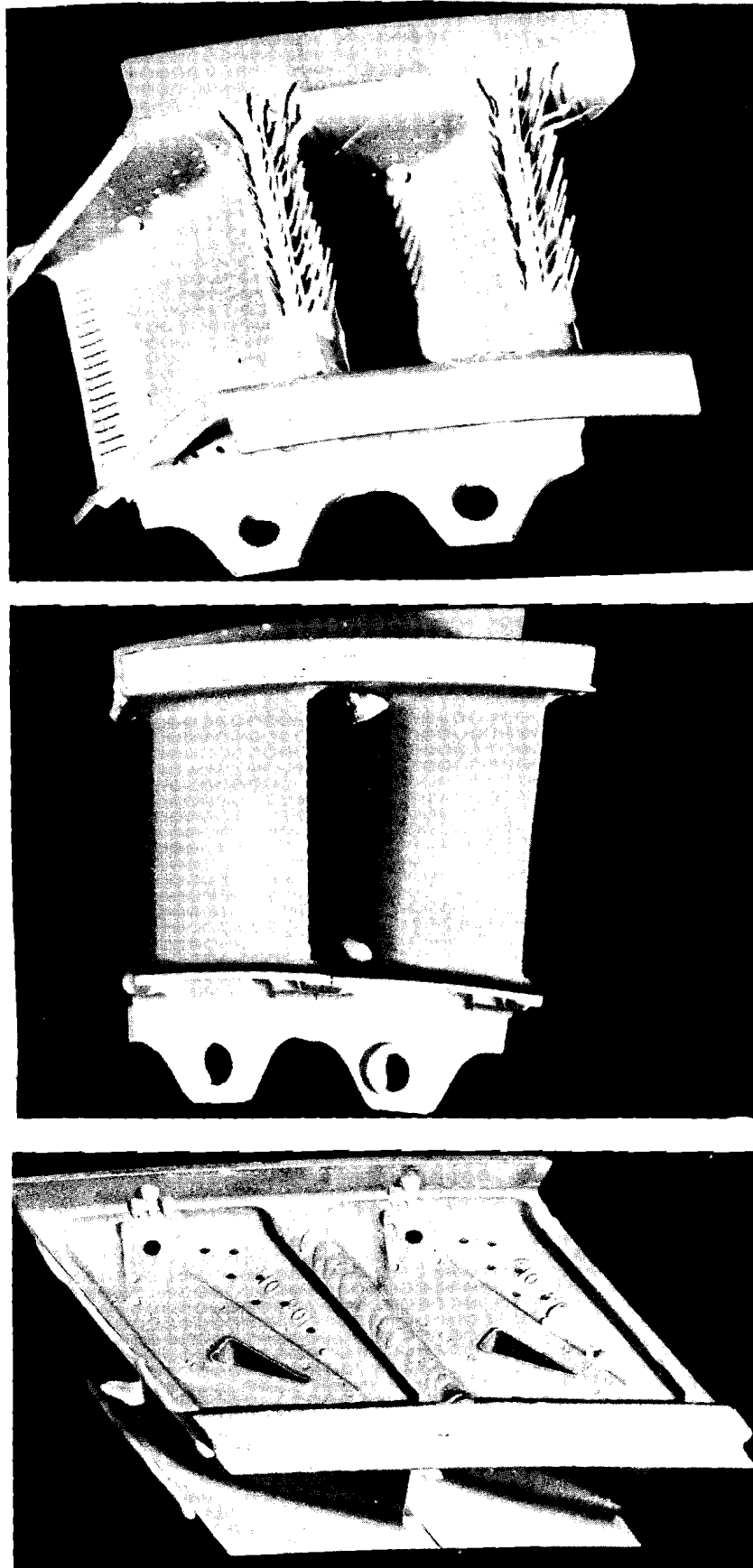
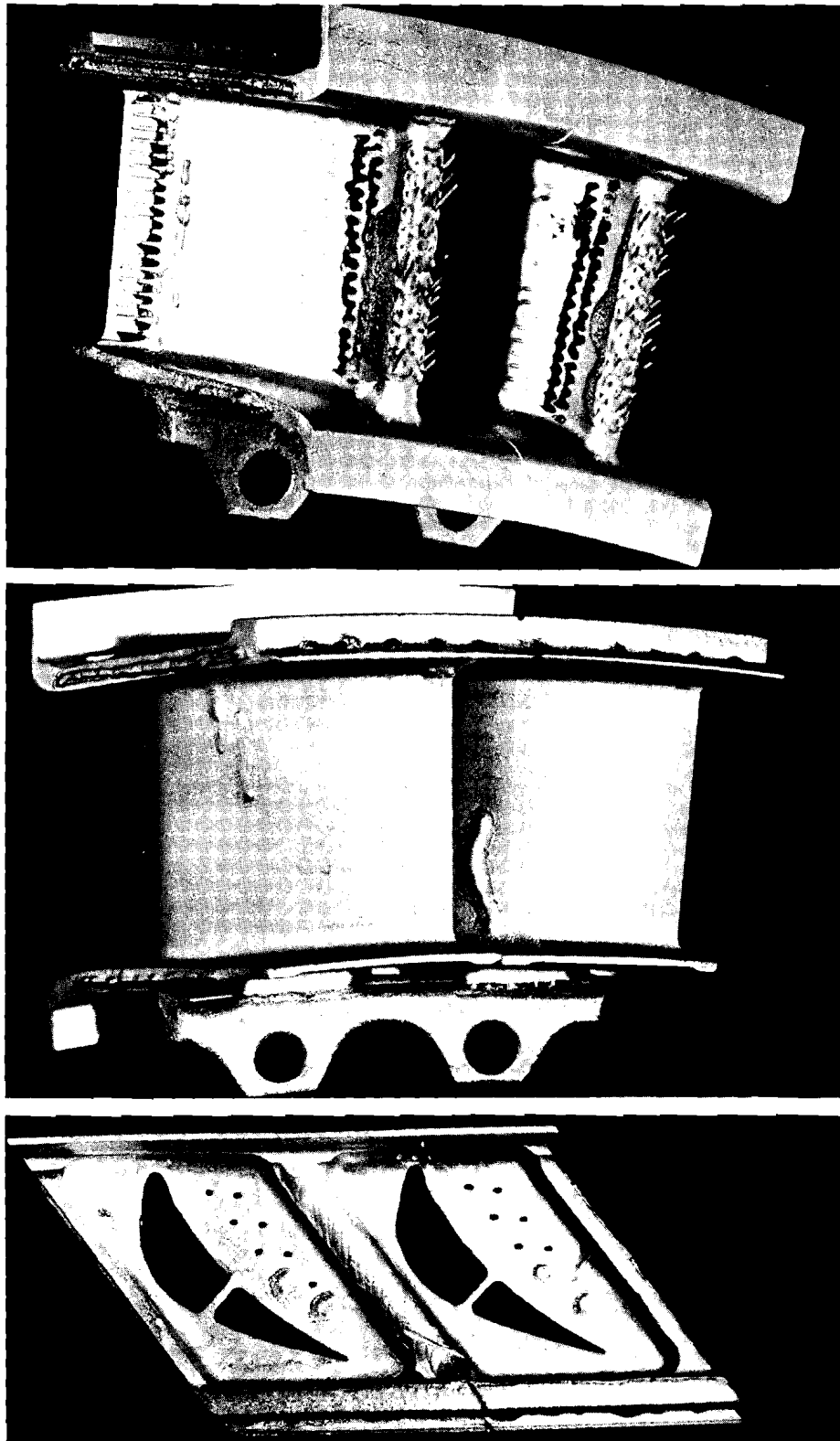
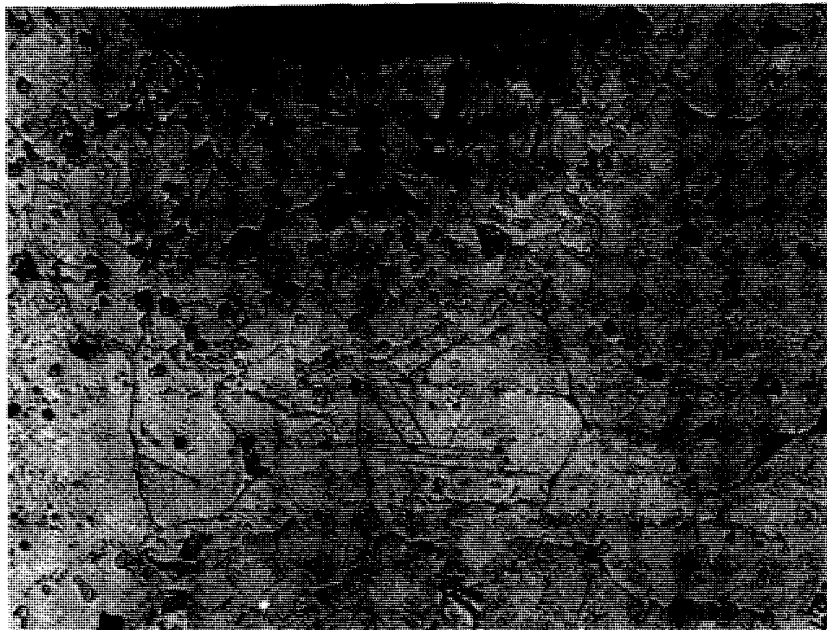


Figure 11. Example of ADH Repair Alloy Application on TF39 Stage 1 HPT Vane

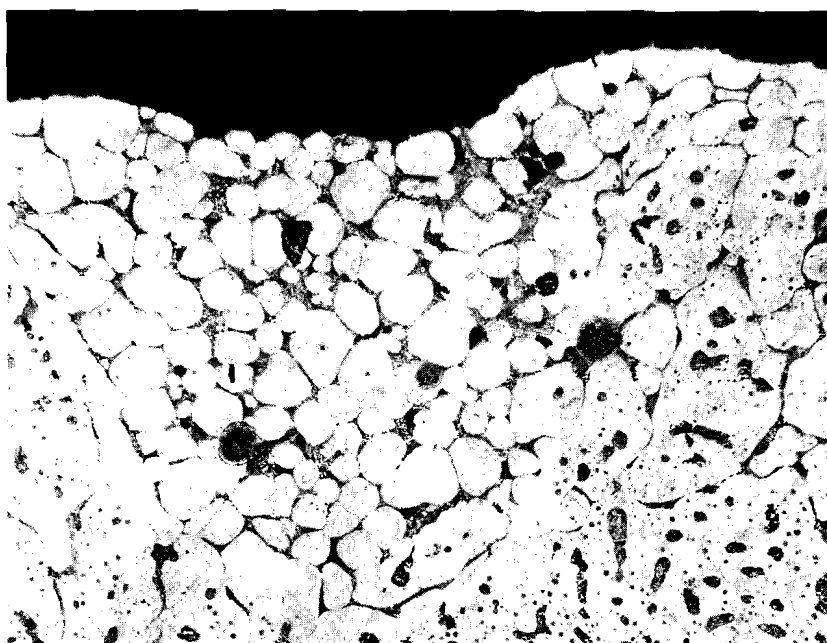


- TOP VIEW - VANE LEADING EDGE. (NOTE QUARTZ PINS IN LEADING
EDGE COOLING HOLES)
- MIDDLE VIEW - VANE TRAILING EDGE (NOTE FLANGE BUILDUP)
- BOTTOM VIEW - VANE OUTER PLATFORM (NOTE FLANGE BUILDUP)

Figure 12. As ADH Repaired Condition of X-40 Engine Run
TF39 Stage 1 HPT Vanes

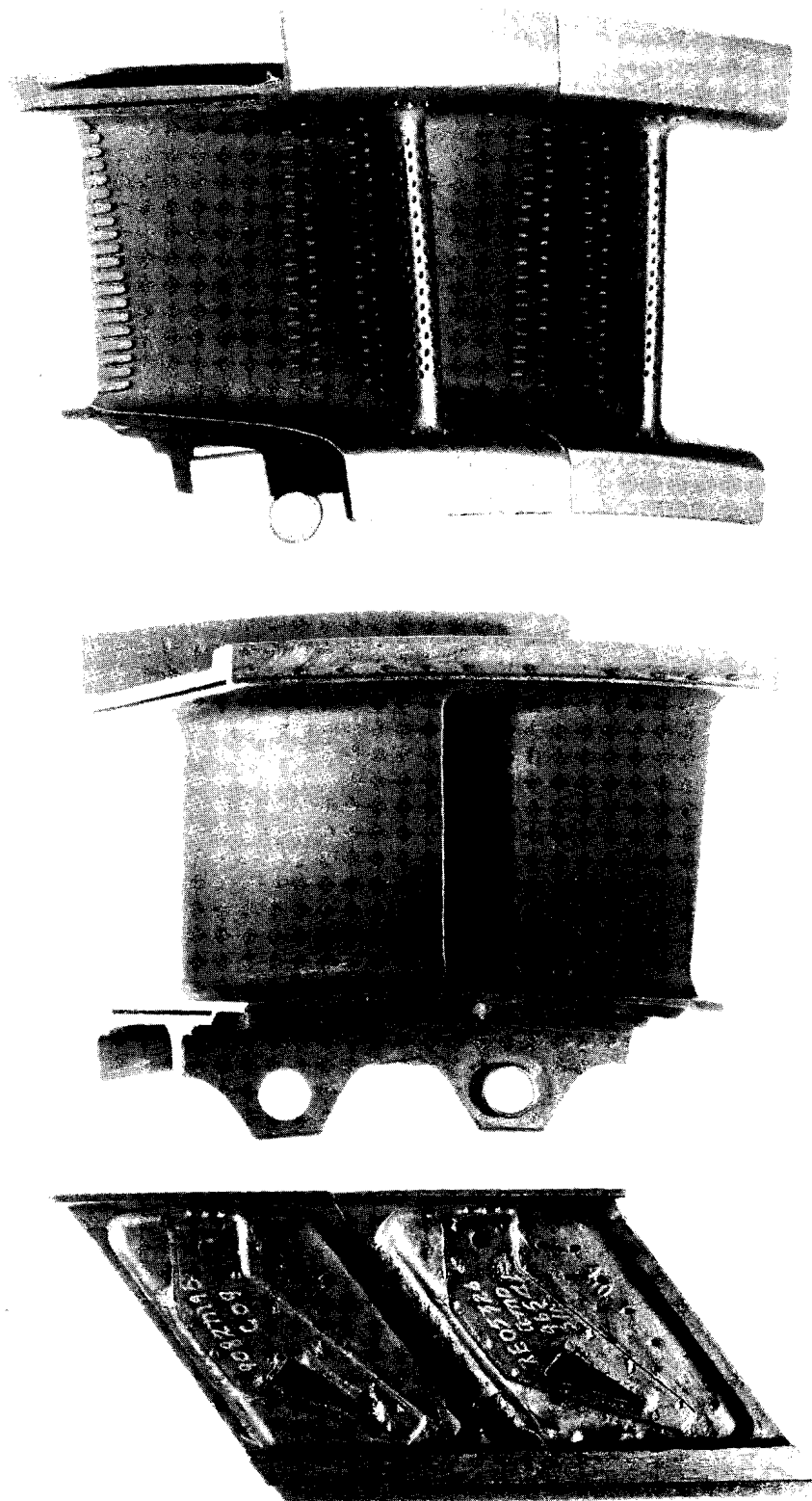


H-33 JOINT IN X-40 MATERIAL



D-15 JOINT IN X-40 MATERIAL

Figure 13. Photomicrograph of ADB Repaired Cracks in X-40 Material



TOP VIEW - VANE LEADING EDGE
 MIDDLE VIEW - VANE TRAILING EDGE
 BOTTOM VIEW - VANE OUTER PLATFORM

Figure 14. Finished TF39 Stage 1 HPT Vane Repaired by the ADH Process

2. TF39 STAGE 2 HPT NOZZLE VANE

Determination of Repair Procedure and Sequence

Prior to using ADH technology for airfoil repair, refurbishment of the stage 2 airfoil was accomplished by TIG welding. Although the Rene' 80 alloy was considered non-weldable, moderate success was achieved by using Inconel 625 filler material and shot peen to leave the weld in compression until heat treat. However, due to the reduced strength properties of Inconel 625, weld repairs were limited to finite length and area. Weld repair also became exhaustive because of the repetitive reweld cycles. Repair part life was also restricted to 1/2 new part life due to deterioration in axial creep properties. After a second weld repair, manufacturing losses ran up to 50%, thus making this repair uneconomical. Weld distortion was a major factor in limiting weld repair area and length. This precluded major refurbishment of mate and fit characteristics because of inability to meet cost goals.

The majority of these problems were overcome and the economics of repair significantly advanced through use of the ADH alloy repair, and this success was primarily achieved through the ability of the fluoride ion source to clean and prepare crack surfaces for wet-out and diffusion of the ADH alloy. The superior properties of the ADH alloy in itself allow a greater repair capability. Crack length, frequency, or location is not a concern with ADH repair. The only restriction is limitation of crack width to a gap size of 0.040 inch. Build-up of worn or fretted surfaces is also possible and may be accomplished on the interstage seals without fear of added dimensional problems.

Inherent weak areas can be strengthened by ADH build-up to increase thickness on areas such as the outboard platform. Burned out surfaces with coating failures are repairable provided no through hole exists. Ideally, an unlimited capability for cost effective repair and refurbishment exists to restore the stage 2 HPT vane sectors through use of the fluoride ion cleaning process and ADH cycle.

Repair Sequence

The initial process sequence identified for repairing the stage 2 vanes can be summarized as follows:

- 1) Inspect for repairability.
- 2) Remark S/N and remove cooling inserts.
- 3) Bench residual braze.
- 4) Strip Codep coating.
- 5) Hot form.
- 6) Dimensional inspect.

- 7) Glass bead clean.
- 8) Fluoride Ion clean.
- 9) Vacuum clean at 2200°F for 2 hours.
- 10) Apply stop-off and ADH alloy.
- 11) ADH braze and diffusion cycle.
- 12) Bench to contour.
- 13) Etch and FP inspect.
- 14) Drill mounting bolt hole.
- 15) Dimensional inspect.
- 16) EDM L/E and T/E holes as required.
- 17) Clean for Codep coat.
- 18) Codep coat.
- 19) Prep braze surfaces for inserts.
- 20) Assemble and alloy inserts.
- 21) Braze and age.
- 22) Visual, waterflow, airflow inspect.
- 23) Mark S/N and final inspect.

The stage 2 HPT vane is cast Rene' 80 with the leading edge cooled by internal impingement air. This air is then used for convention cooling of the mid-chord region and is discharged through holes in the trailing edge and inner band.

Typical service induced distress is shown in Figure 15. Standard repair procedures call for weld repair with Inco 625 filler. Areas of weld repair are limited in length and location due to (1) low weldment strength relative to the Rene' 80 parent metal, (2) weld distortion, and (3) cracking tendencies of the parent alloy. On a survey sample of 1450 vanes inspected, 37% had defects in excess of the then current weld repair limits.

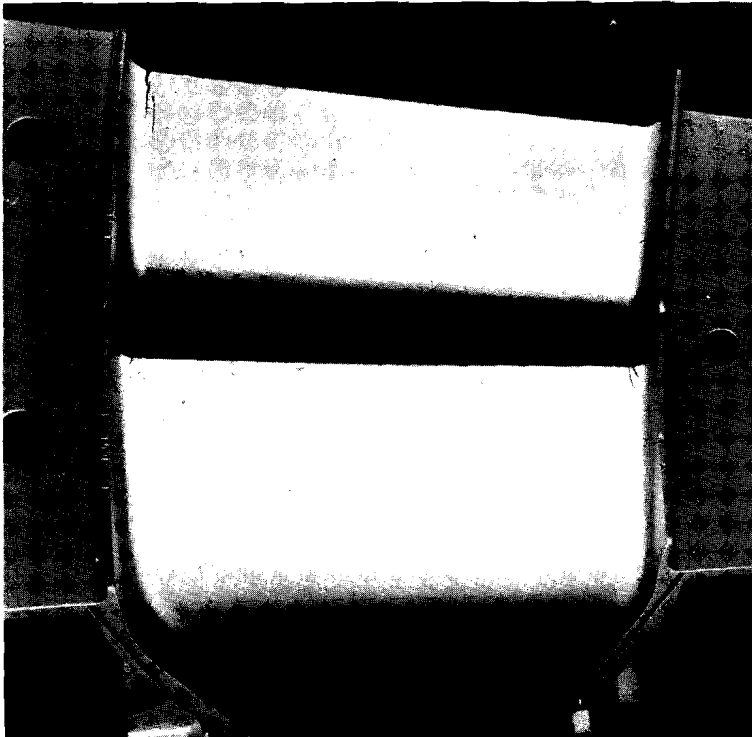
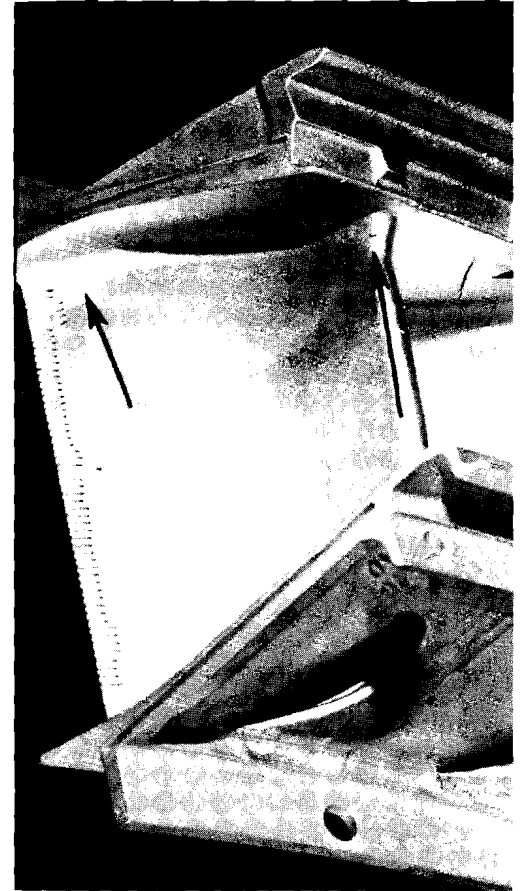
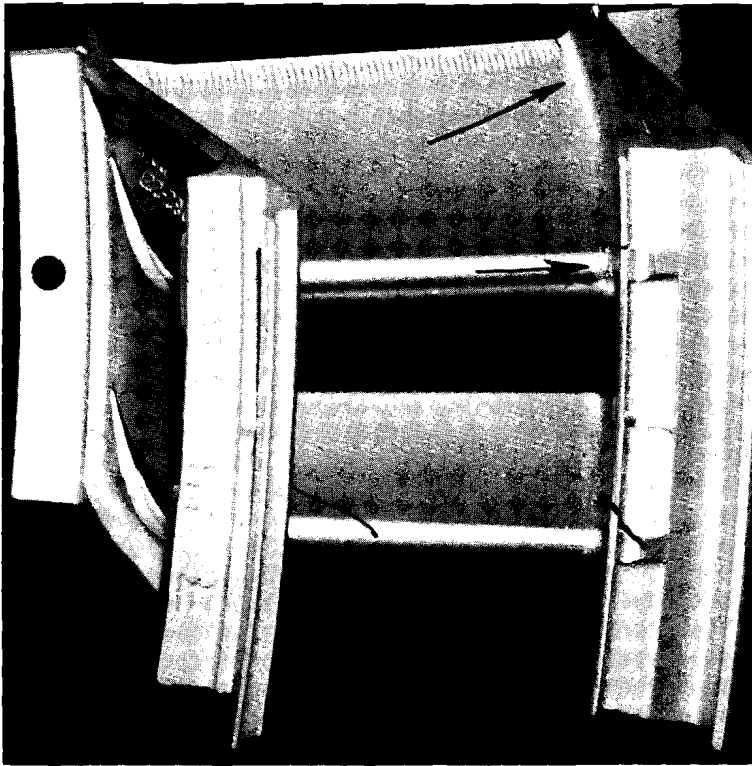


Figure 15. Appearance of Engine Run TF39 Rene' 80 Stage 2 HPT Vanes After Grit Blast Clean

The goals established for ADH repair were extended to cracks up to 0.040" wide and it was anticipated that this would increase the total of repairable parts in excess of 90%. As with stage 1 vanes it was felt that zone alloying was a more cost effective method for repair of individual cracks than individual crack identification and alloy application. The two significant operations which then required extensive evaluation for process application and substantiation were the fluoride ion cleaning process and the ADH alloy selection and evaluation.

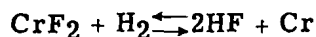
Fluoride Ion Cleaning

The gaseous cleaning medium containing the active fluoride ion was developed to remove the complex aluminum and titanium containing oxides from airfoil cracks greater than 0.001" wide, cooling holes, and all other surfaces.

Process Fundamentals

The basic chemical reactions which occur during fluoride ion cleaning are depicted in Figure 16. At low temperature, near 500°F (260°C), ammonium fluoride (NH₄F) combines with chromium (Cr) powder to produce chromium fluoride, CrF₂. The gaseous by-product of this reaction is ammonia, NH₃, which decomposes into nitrogen and hydrogen upon contact with the metallic surfaces of the reaction box. These gases purge the box of residual air and provide hydrogen for subsequent reaction with the CrF₂.

At temperatures above 1200°F (650°C), the chromium fluoride, CrF₂, reacts with hydrogen to produce the active cleaning agent, HF gas. Since chemical equilibrium is maintained within the cleaning retort, the HF concentration is directly related to the equilibrium constants for the equation:



K. Jellinek and A. Rudat⁽²⁾ reported values for the equilibrium constant $\text{Ln } K = \frac{P^2(\text{HF})}{P(\text{H}_2)}$ as plotted in Figure 17. If, it is assumed that $P(\text{HF}) + P(\text{H}_2) = 1$ atmosphere, the extrapolated values of $P(\text{HF})$ as a function of equilibrium temperature may be plotted as shown in Figure 18.

Based on these data, it is evident that HF concentration exhibits rapid change as process temperatures are increased up to 1800°F (980°C). Above 1800°F (980°C) the process becomes controllable with a HF concentration of 24 to 27 percent. Above about 1870°F the partial pressure of CrF₂ becomes significant with melting occurring at 2012°F (1100°C).

Thus, from the viewpoint of process control there is a relatively narrow temperature range above 1800°F where the HF concentration remains within predicted limits. Also, because the amount of HF gas present depends on this equilibrium reaction, the process retort must be semi-sealed to prevent loss of the CrF₂ source by excessive hydrogen introduction.

2. Jellinek, K. and Rudat, A., Zeit. Anorg. Chem., 175, 281, 1928.

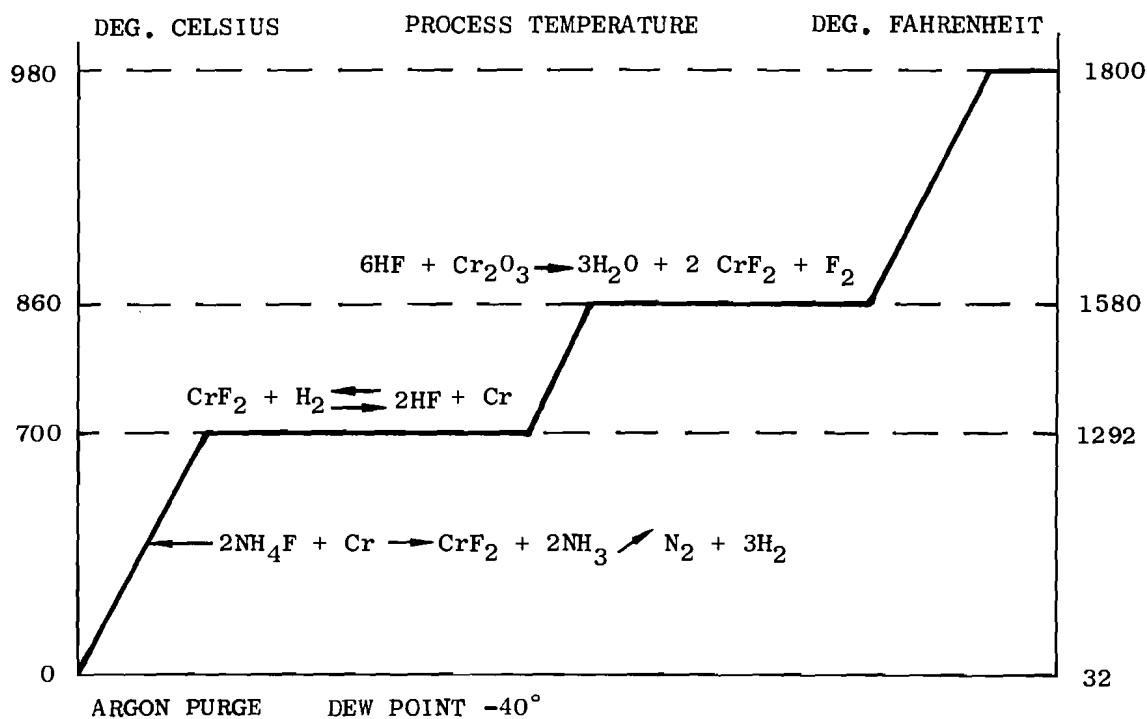


Figure 16. Chemical Reactions During Cleaning in a Stable Fluoride Reducing Atmosphere

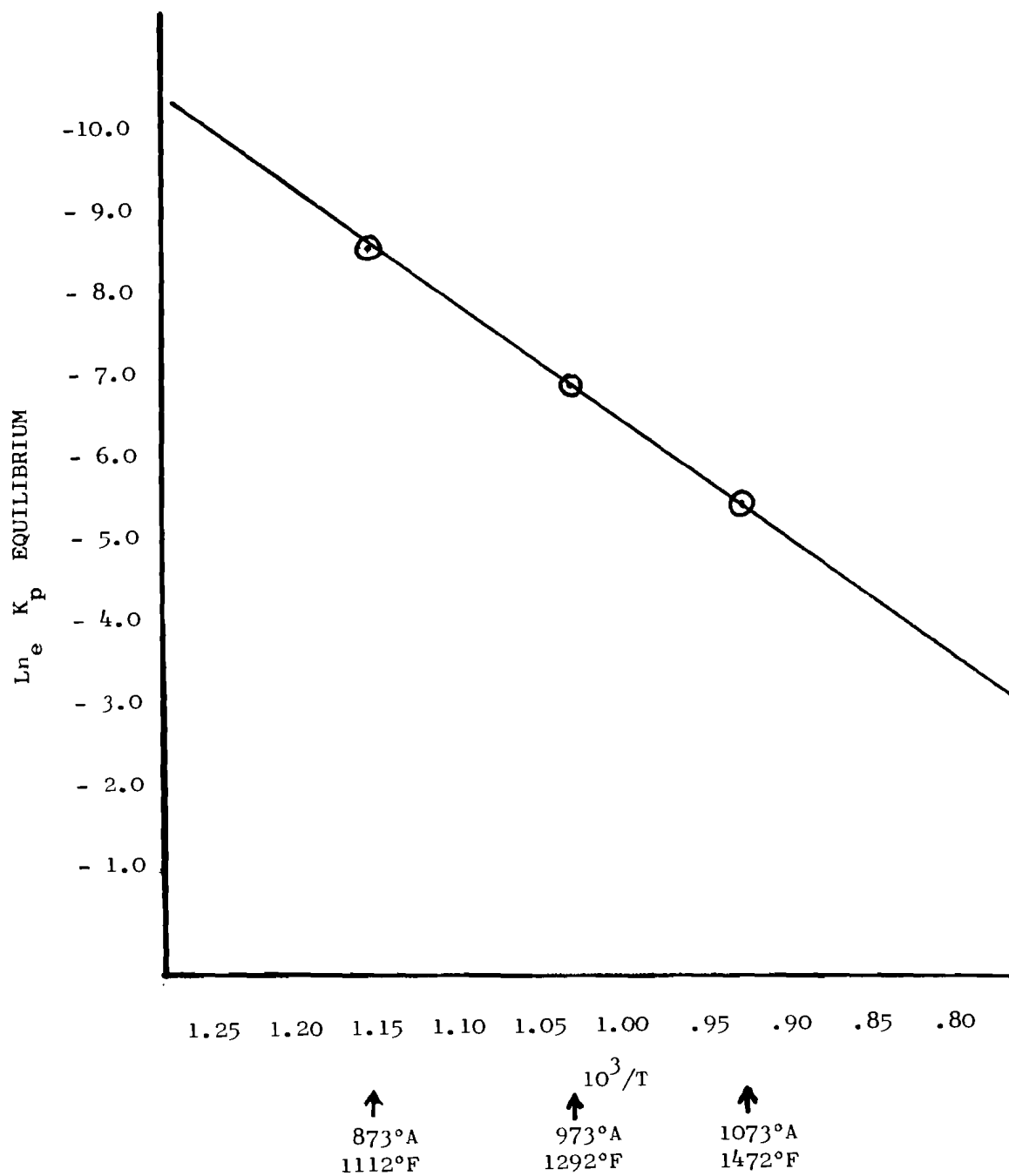


Figure 17. Equilibrium Constant $K_p = \frac{p^2(\text{HF})}{p(\text{H}_2)}$ Versus Temperature
for Equation $\text{CrF}_2 + \text{H}_2 \rightleftharpoons \text{Cr} + 2\text{HF}$

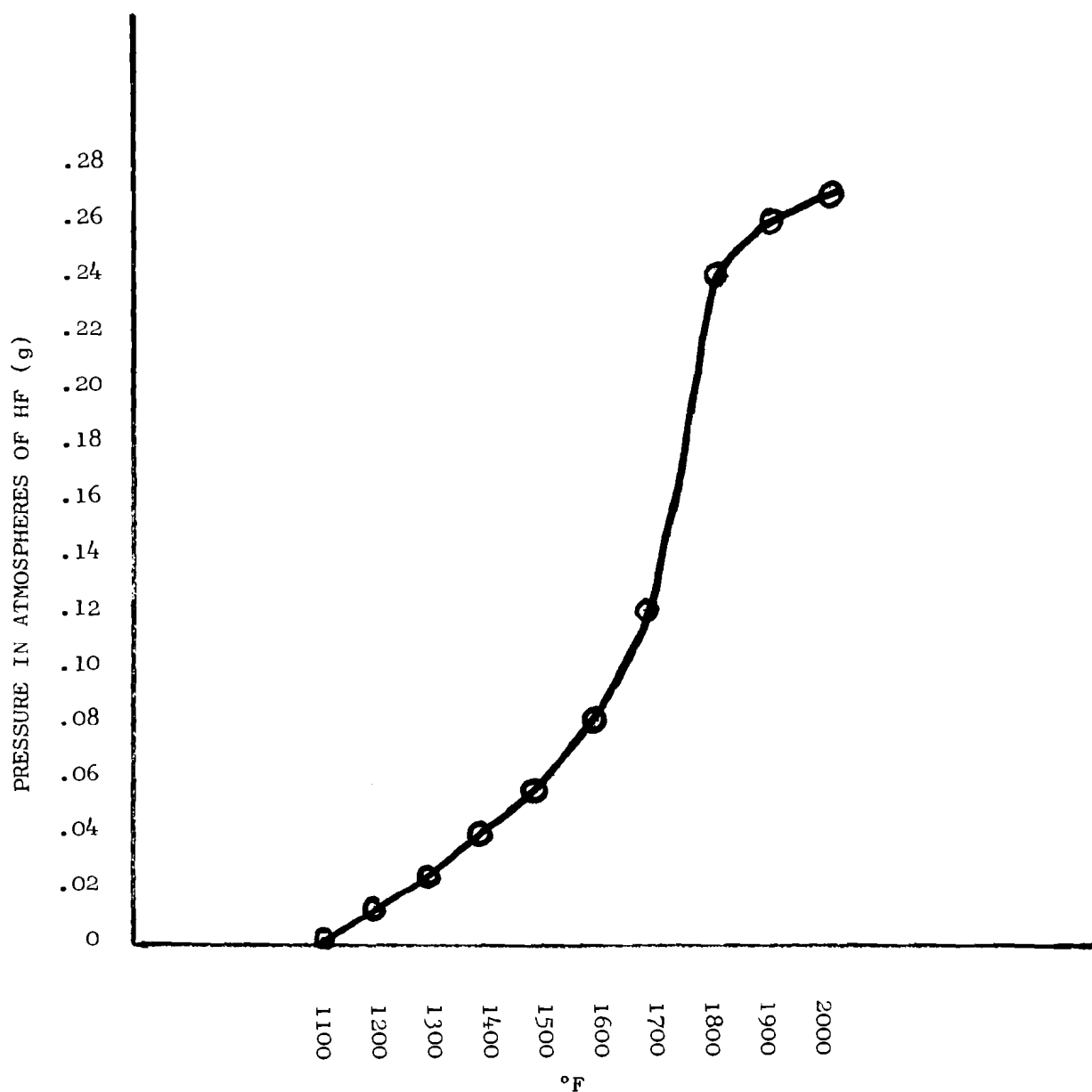
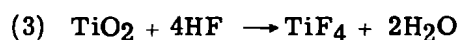
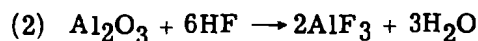
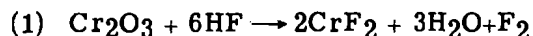


Figure 18. HF (g) Pressure Variation with Temperature in the Equilibrium Reaction of
 $\text{CrF}_2 + \text{H}_2 \rightleftharpoons \text{Cr} + 2\text{HF}$ (Assumed $P(\text{HF}) + P(\text{H}_2) = 1$)

As the process temperature is increased above 1600°F (870°C) the oxides of chromium, titanium and aluminum are transformed by the theoretical chemical equations:



On superalloys, oxides are present as complex spinels containing aluminum and titanium. The effect of fluoride ion on real oxides present within cracks is shown in Figure 19. Oxide removal is complete, except for a small amount at the crack tip. These residual defects are considered acceptable by repair design engineering since their size is similar to normal defect limits for vane castings.

Statistical Studies of Process Parameters

The process has been evaluated for its ability to clean oxides from the surfaces of engine run hardware. These studies were conducted by a statistical program evaluating time, temperature, concentration of NH_4F or CrF_3 as the F^- source and H_2 and Argon as carrier gases. (CrF_3 used in this program was actually the hydrated form $[\text{CrF}_3 \cdot 3 \frac{1}{2} \text{H}_2\text{O}]$ but is shortened for simplification in later use.) Table 3 shows the various conditions used in this statistical evaluation.

The primary acceptance requirements were braze flow after cleaning of the oxides on the surface and the amount of IGA on the Rene' 80.

TABLE 3
PROCESS PARAMETER EVALUATION
FOR FLUORIDE ION CLEANING

<u>Run</u>	<u>Temperature (°F)</u>	<u>Time (Min)</u>	<u>F⁻ Source</u>	<u>Weight (GMS)</u>	<u>Carrier</u>
1	1600	30	NH_4F	100	None
2	1600	30	NH_4F	100	H_2
3	1600	30	CrF_3	100	H_2
4	1600	30	NH_4F	100	Ar
5	1800	60	NH_4F	200	H_2
6	1800	60	CrF_3	100	H_2
7	1800	60	CrF_3	200	Ar
8	1800	60	NH_4F	100	Ar
9	1800	30	CrF_3	200	H_2
10	1800	30	CrF_3	100	Ar
11	1600	30	CrF_3	200	Ar
12	1600	60	CrF_3	100	Ar
13	1600	60	CrF_3	200	H_2
14	1600	60	NH_4F	100	H_2
15	1600	30	NH_4F	200	H_2
16	1800	30	NH_4F	100	H_2
17	1800	30	NH_4F	200	Ar
18	1600	60	NH_4F	200	Ar
19	1600	240	NH_4F	200	H_2



5



50X

Figure 19. Photomicrograph of Rene' 80 Airfoil Crack After Fluoride Ion Cleaning at 1800°F/1 Hr

Previous runs at 2000°F produced IGA up to 0.010 inch in depth and alloy depletion up to 0.005 inch using CrF_3 . Although the 1600°F process showed less attack, oxides were removed to a lesser extent as determined by braze flow. This is probably due to the lower concentration of the HF gas. The braze flow studies indicated that 1800°F with either NH_4F + Cr powder or CrF_3 cleaned the surface effectively enough to permit complete flow of the brazing alloy on the prior oxidized surface. The CrF_3 was readily available commercially and thus was selected as the fluoride ion source.

This analysis also showed that either argon or H_2 could be used as a carrier gas, although hydrogen resulted in a cleaner appearance.

To complete the process, a subsequent vacuum heat treat is required to remove any excess metal fluorides that may be present on the cleaned material. This is accomplished by taking the airfoil to its solution temperature (for Rene' 80, 2200°F, 2 hr).

Although surface oxides can be removed successfully by the F^- cleaning, occasionally the very tight tip of a crack that is less than 0.001 inch in width cannot be totally cleaned of all oxides. This is because the gases are not coming in intimate contact with the metal oxide. This was shown in Figure 19.

For successful repair, cracked engine components require adequate cleaning procedures and a bonding alloy compatible with the airfoil alloy.

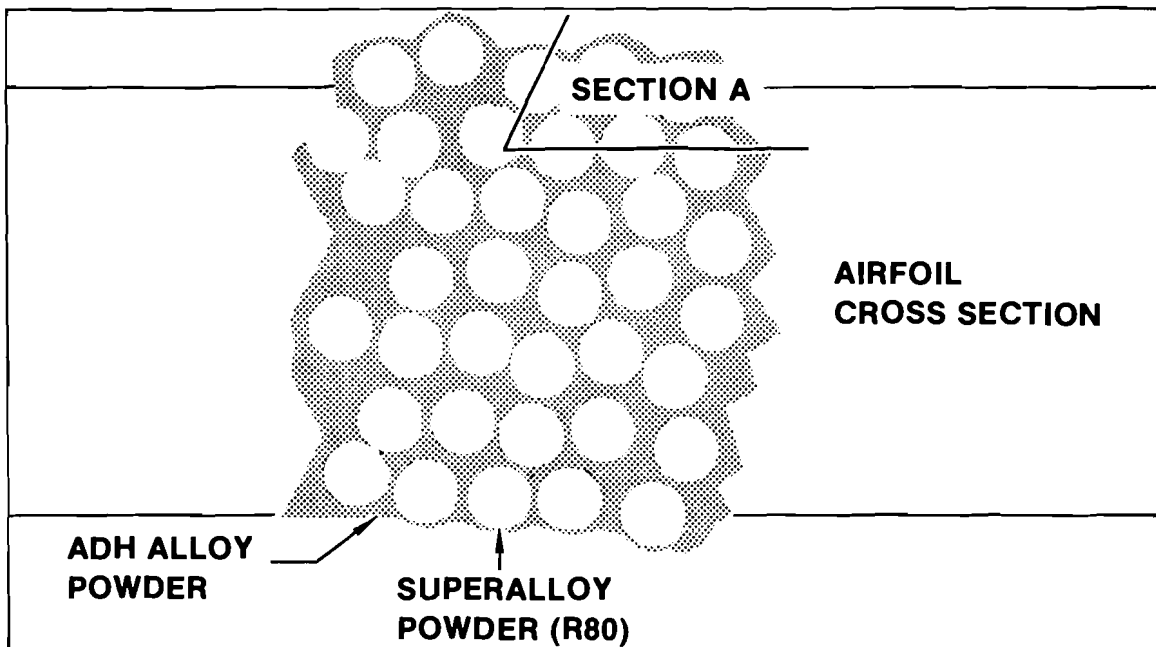
Activated Diffusion Healing

Process Fundamentals

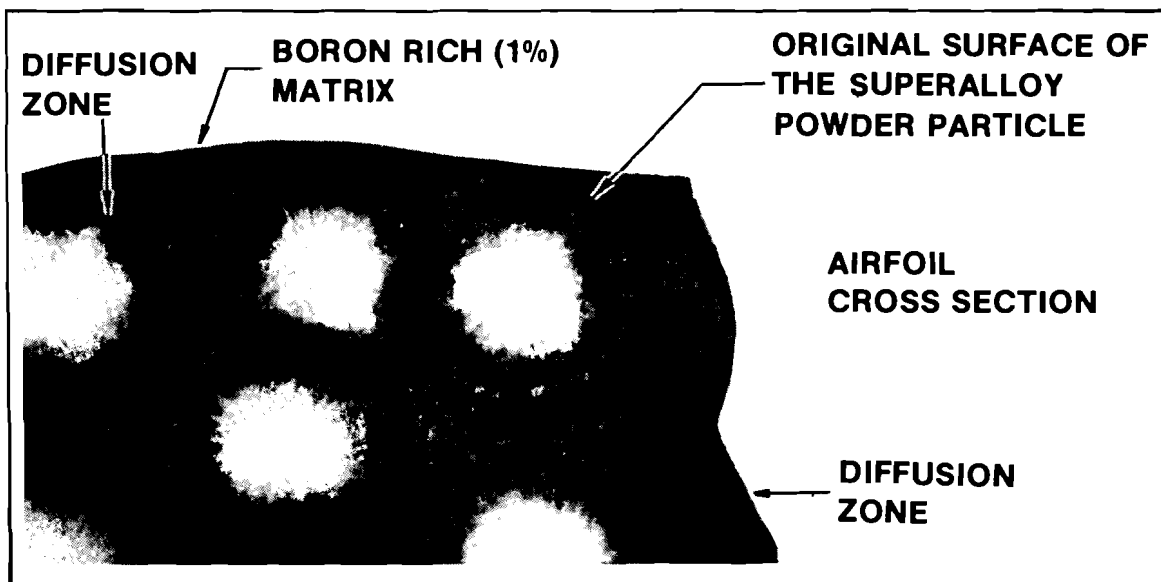
The activated diffusion healing (ADH) process developed by the General Electric Company incorporates the use of alloy powders matched to the composition of the airfoil alloy and mechanically blended with an activated diffusion bonding (ADB) alloy.

The purpose of this combination is to, in effect, fill the large cracks so as to cast with an alloy that would at one temperature, melt, diffuse, and solidify in the crack and develop properties comparable to the airfoil material. This technique is shown graphically in Figure 20. This illustration shows the larger superalloy particles surrounded by small ADB alloy particles thereby resulting in a relatively high density mixture.

Upon reaching liquification temperatures, the ADB alloy first melts and then diffuses simultaneously into both the superalloy powder and the superalloy airfoil. Solidification occurs isothermally. The result is a casting with basically the same chemistry as the airfoil alloy (with an increase in boron content $\approx 1.2\%$). As expected some porosity/voiding will occur, however, the strength level of this type of filler is greater than an equivalent Inco 625 weld repair. Figure 21 shows an ADH repaired crack with minimal voiding and some oxide remaining in tight crack areas even after fluoride ion cleaning.



GRAPHIC DEMONSTRATION OF THE LIQUID PHASE SINTERING PROCESS PRIOR TO "CASTING"



GRAPHIC "BLOW-UP" OF SECTION A AFTER CASTING

Figure 20. Graphic Illustration of Liquid Phase Sintering Before and After Casting

Figure 21. Rene', 80 C
at 1800°F/



This type of alloy mixture is also being used for constructing fillets or for filling large gaps when total section replacement is necessary. The concept is similar to that of wide-gap brazing patented in 1963 by the General Electric Company. (U.S. Patent 3,079,269.)

ADH Alloy Selection

The criteria for selection of any ADH filler material required for optimum repair of cracks, pits, erosion, and worn metal includes:

- 1) Flow and wetting action characteristics.
- 2) Tensile shear strength.
- 3) Nil-strength temperature - the minimum temperature at which the joint is unable to sustain a small steady-state load.
- 4) Impact strength.

A fifty-fifty mixture of D-15 and Rene' 80 powder by weight was used as a filler material for Rene' 80 bonded at 2200°F for thirty minutes followed by diffusion heat treatment which consisted of:

- | | |
|-----------------|-----------------|
| a) 2000°F/2 hrs | c) 2175°F/2 hrs |
| b) 2100°F/2 hrs | d) 2000°F/4 hrs |

and then the standard Codep coat cycle of 1925°F/4 hrs and age at 1550°F/16 hrs. To assess joint efficiency, the following type tests were conducted: Room temperature tensile, impact, and nil-strength of the bond joint. Testing was conducted on specimens machined from 0.060 inch thick cast Rene' 80. Additionally tensile shear specimens were manufactured in a manner previously described.

The average results of three tests pulled at 2000#/min. load rate were 34.5 ksi for the R80/D15 ADH alloy. In each test, failure occurred in the R80 base metal at the edge of the bond line. Figure 6 illustrates a typical failure.

To assess the over-temperature capability of D-15/Rene' 80 bonded joints in Rene' 80, the "Nil-Strength temperature" was established. This was accomplished by loading 2T overlap shear joints after full heat treatment with 125 psi load and increasing the temperature from 1900°F in 50°F increments until the shear joint failed. The lowest temperature at which the load failed was 2200°F. As a comparison, Rene' 80 base metal will fail in the same test at approximately 2350°F.

Pendulum impact testing was conducted on specimens from 0.060 inch cast Rene' 80. The impact specimens were machined 1.5 inch long by 0.5 inch wide with a bond joint gap from 0.003 inch to 0.040 inch. The impact was directly on the joint. For comparative data, Rene' 80 parent metal specimens were machined to the same configuration. Table 4 shows the test results.

Additional mechanical property testing performed to determine 1600°F low cycle fatigue strength indicated that:

TABLE 4
PENDULUM IMPACT PARENT METAL TESTS

	<u>Width At Impact</u>	<u>Material Thickness</u>	<u>Failure Load</u>
Rene' 80	.480	.064	7.03 Ft-Lb
	.469	.066	5.94 Ft-Lb
	.465	.066	9.47 Ft-Lb
	.476	.068	8.57 Ft-Lb
	.481	.067	8.53 Ft-Lb
	.471	.071	7.51 Ft-Lb

PENDULUM IMPACT TESTS (Rene' 80 Material -
Rene' 80/D-15 Bonding Alloy 50/50 Mix - Flat Sheet)

<u>Gap of Bond Joint</u>	<u>Width at Joint</u>	<u>Thickness of Joint</u>	<u>Failure Location</u>	<u>Failure Load Ft/Lb</u>
.003 inch gap	.475	.060	J	3.60
	.450	.060	J	1.79
	.444	.065	J	1.33
	.477	.065	J	0.96
	.459	.057	P	3.42
	.467	.057	P	4.19
.010 inch gap	.449	.065	J	1.20
	.475	.065	J	1.84
	.480	.070	P	6.98
	.452	.070	J	2.56
	.471	.062	J	3.64
	.452	.062	J	2.99
.020 inch gap	.470	.059	J	1.49
	.457	.059	J	1.31
	.478	.060	J	4.29
	.448	.060	J	2.30
	.472	.061	J	1.43
	.448	.061	J	3.79
.040 inch gap	.475	.060	J	2.07
	.453	.060	J	1.78
	.480	.066	J	1.63
	.437	.066	J	1.85
	.441	.061	J	0.98
	.478	.061	J	1.69

P = Parent Metal Failure

J = Bond Joint Failure

- 1) There is little effect on parent metal strength caused by the repair ADH cycle. Effect of gap width is negligible on ADH strength. Joint efficiency is 80%.
- 2) There is a 10% reduction in rupture strength due to the repair cycle. Gap width does show effect on rupture strength, however values obtained are superior to Inco 625 repair weld procedure.
- 3) There is a 20% reduction in LCF strength and effect of gap width was not found to be significant.

These data are presented graphically in Figures 22 through 24.

Scale-Up of Repair Process

During the scale-up effort scrap vanes with existing engine induced cracks were used to verify the cleaning effectiveness of F⁻ cleaning. After each run, cracks were broken open and cleanliness verified by visual and SEM analysis (Figure 25). Although this was desirable for the initial efforts this type of analysis was impractical for service shops.

A Rene' 80 control coupon shown in Figure 26 was used as a quick means for determining the effectiveness of the F⁻ cleaning run. Coupons were preoxidized at 1950°F for 16 hours in air prior to cleaning. The degree of cleaning was determined by visual measurement of the clean area on the side extending radially from the five drilled holes. At least 0.020 inch of peripheral cleaning around each hold was required to assure satisfactory part cleaning. Although used with some success, it is felt that other coupon designs may more nearly represent a crack configuration and provide a measure of cleaning effectiveness for subsequent ADH repair.

During transition trials for scale-up of the identified repair process, preliminary results of CF6 engine tests became available. Several CF6 stage 2 HPT vanes had been processed in the laboratory by the F⁻ clean and ADH process with the D-15/R' 80 50-50 mix. These components were run for 1000 "C" cycles along with comparison vanes representing: (1) the current weld repair, (2) engine run used parts, and (3) new parts. Post-test evaluations showed that the ADH vanes exhibited airfoil distress to a much greater extent than any of the comparison vanes. The distress was in the form of cracking primarily on the airfoil pressure side at the aft end of the internal cavity and to a lesser extent, on the airfoil leading edge. These are known distress areas on the stage 2 vanes. Figure 27 shows the most severe condition of the engine tested vanes. Metallographic examination revealed catastrophic oxidation in areas where the Codep coating was cracked or damaged. Figure 28 illustrates the severity of oxidation attack. Microprobe and microscopic examination of the microstructure at the substrate/diffusion zone interface indicated severe alloy depletion with a decrease in gamma prime and MC carbide content to a depth of approximately 0.006". The extent of all microstructural changes appeared to be related to the prior thermal exposure of the parts as the changes were more severe in the area of the vanes that operate at the highest temperature. Especially encouraging was minimal cracking in the repaired regions of vanes. This cracking seemed to be a random occurrence rather than associated with prior cracks. Further evaluations indicated the presence of Kirkendall voids beneath the Codep coating of F⁻ cleaned/ADH repair and Codep coated parts.

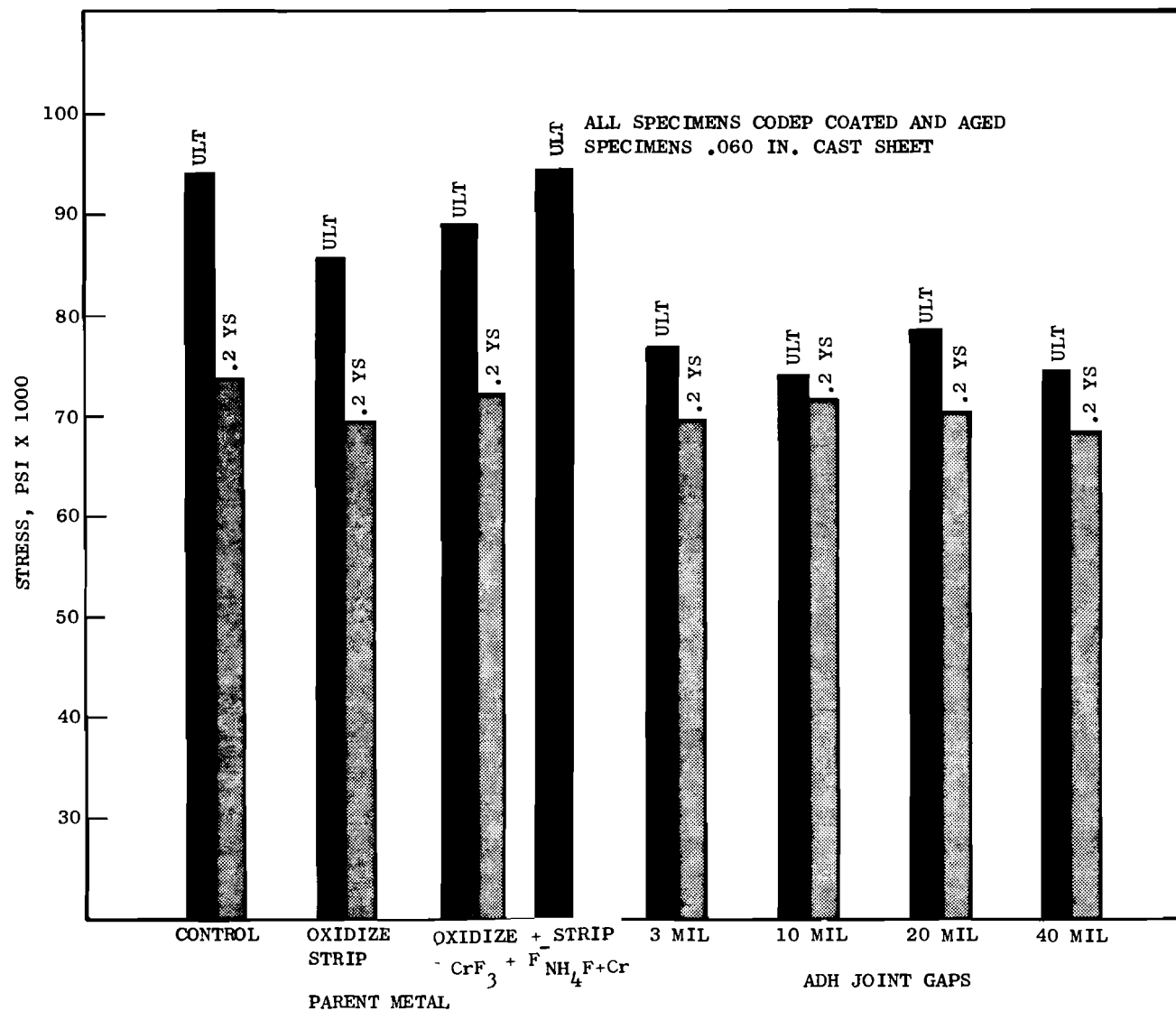


Figure 22. Rene' 80 1600F Tensile Strength

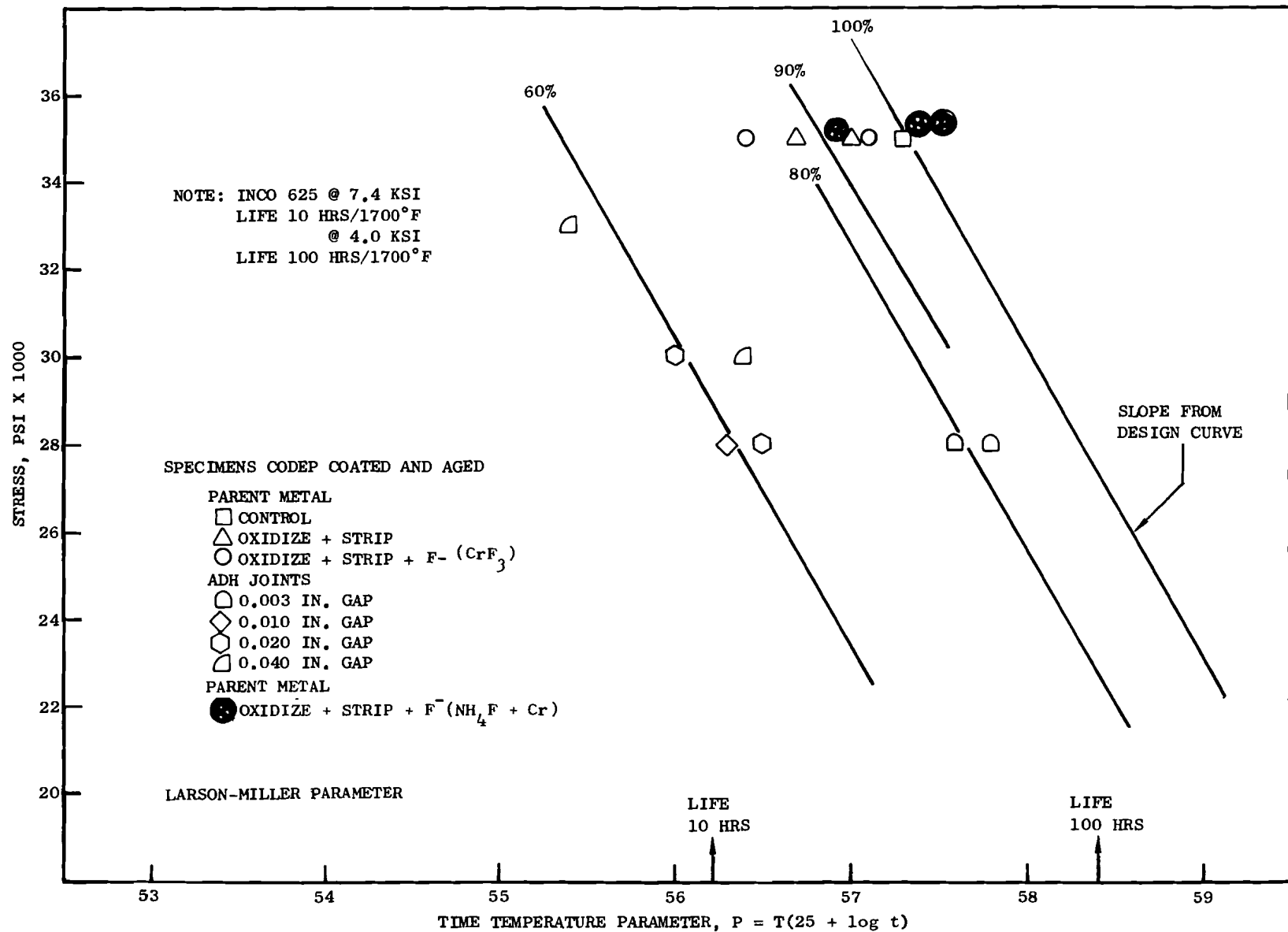


Figure 23. Rene' 80 1700F Stress Rupture Life

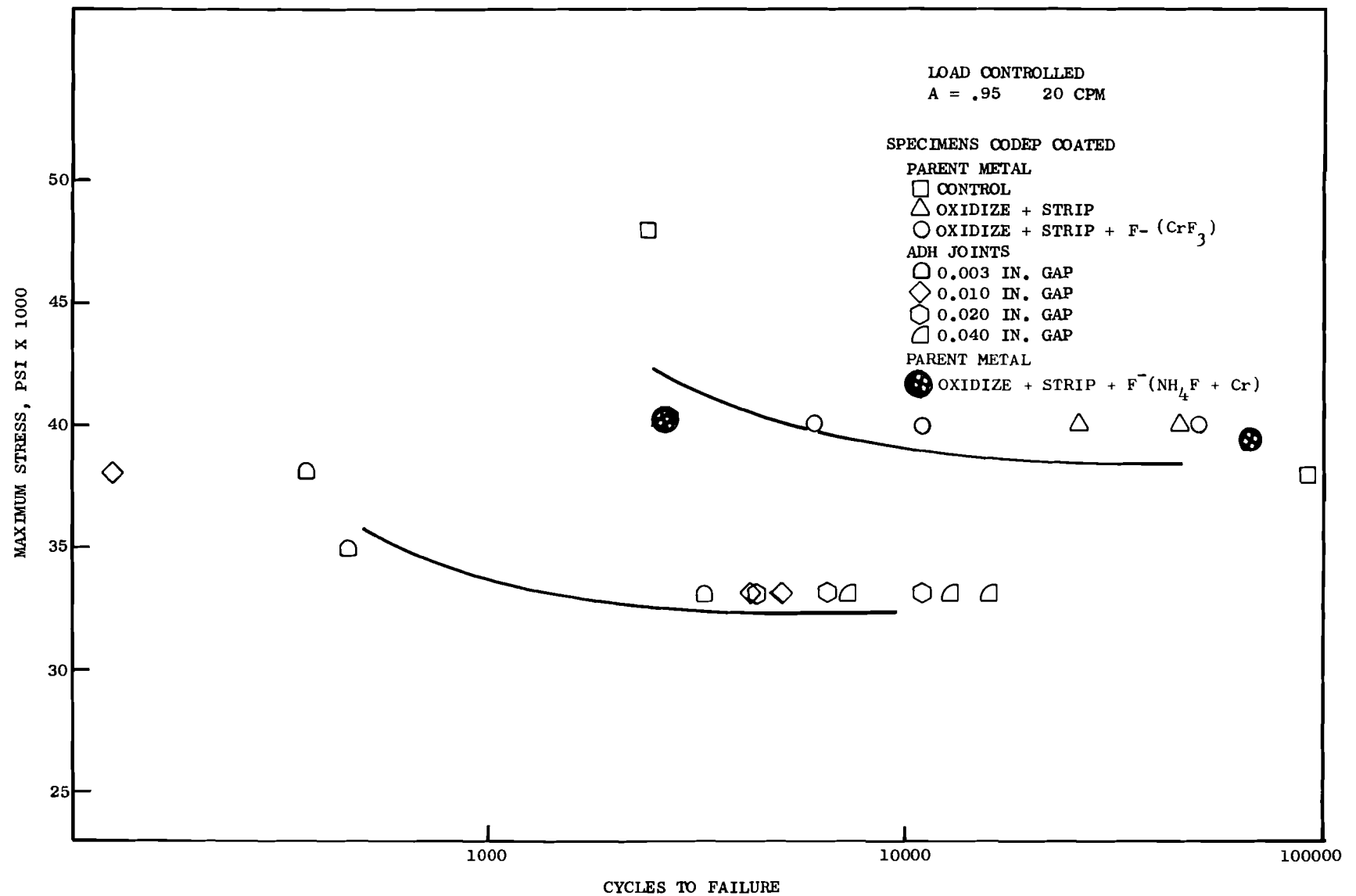
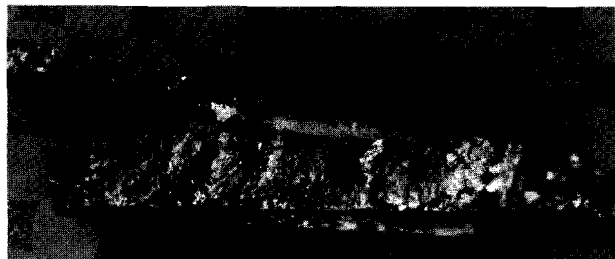
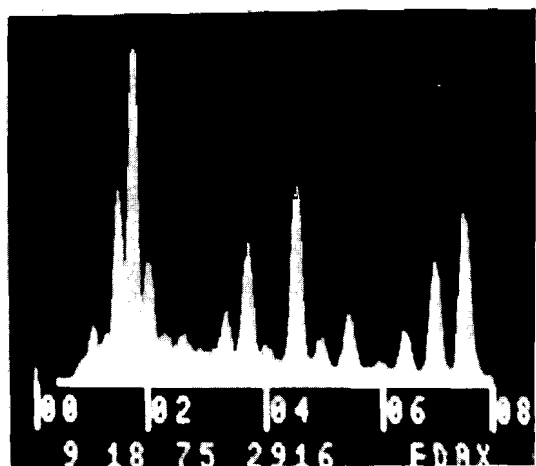


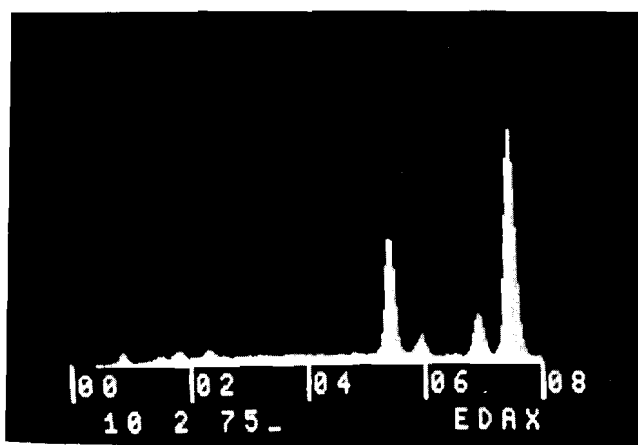
Figure 24. Rene' 80 1800F Low Cycle Fatigue Life



RENE' 80 CRACK SURFACE APPEARANCE. LEFT: AS ENGINE RUN,
RIGHT: FLUORIDE ION CLEANED



OXIDIZED



CLEANED

Figure 25. SEM Analysis of Rene' 80 Crack Surface Before and After
Fluoride Ion Clean

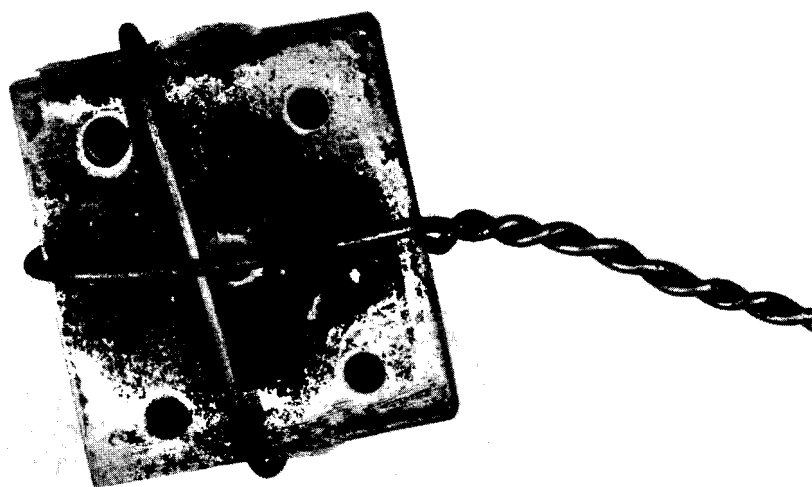


Figure 26. Rene' 80 Control Coupon for Effectiveness of F-Cleaning

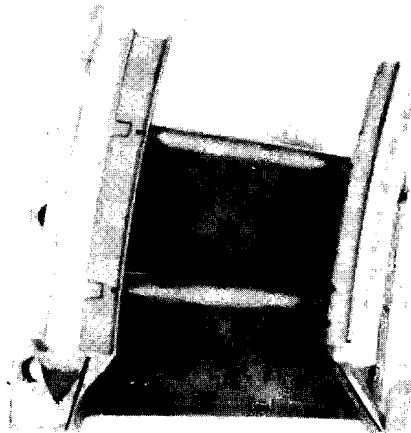
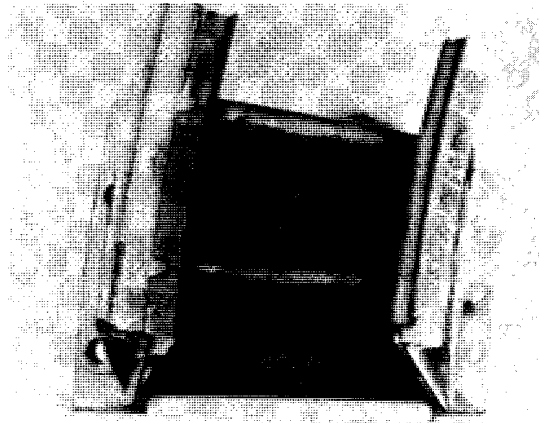
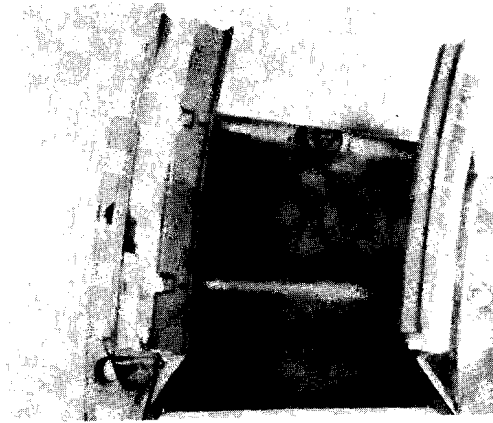


Figure 27. Stage 2 vanes after 100 cycles engine test. All three parts had been stripped F-Cleaned at 1800°F w/CrF₃ plus 2200°F/2 hrs in vacuum, then ADH repaired and CODEP coated.



Figure 28. Fluoride Ion Cleaned Vane After 1000 Cycles Engine
Test 500x

A controlled process evaluation was initiated to study this phenomena. Kirkendall voids were not observed immediately after the F⁻ cleaning portion of the process; however, after both subsequent vacuum clean and/or Codep coating, they were observed. This indicated that a diffusion mechanism became operative during the subsequent thermal exposure and affected a rapid diffusion of substrate elements to the alloy depleted surface leaving the observed Kirkendall voids. The oxidation characteristics of the resulting surfaces are shown in Figure 29 along with the normal oxidation of R80 on a stripped and oxidized component. The depleted alloy layer left by F⁻ cleaning and subsequent oxidation testing resulted in catastrophic oxidation attack. Additional thermal exposure in the vacuum clean cycle allowed more diffusion and thus reduced the amount of oxidation attack.

This study indicated that it was necessary to remove this alloy depleted layer after F⁻ cleaning and both chemical and mechanical means were utilized to affect this metal removal. Figure 30 shows a vane segment which had 0.001" chemically removed from the surface after F⁻ cleaning and even though the Codep coating has failed (cracked), there is no oxidation attack of the diffusion zone/substrate interface. A mechanical method of metal removal was also used and after some evaluation was included as part of the established process.

Inconsistency in cleaning effectiveness was noted in the scale-up to usage of larger quantities of CrF₃ which was probably attributable to excessive amounts of moisture present. As a result of this, full emphasis was placed on utilizing the NH₄F plus chromium powder as a fluoride ion source to scale-up the process from the original set of statistical runs.

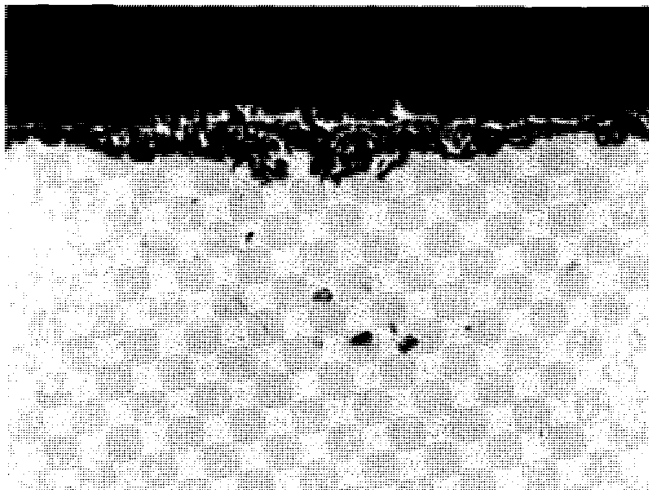
Additional tests were conducted to make some check points on the NH₄F cleaning process. Figures 31 and 32 show that F⁻ cleaning with NH₄F and Cr powder has less effect on degrading the Rene' 80 surface. The addition of the dehusk operation provided a contribution to the overall oxidation results after subsequent Codep coating and should be noted in these photomicrographs.

Mechanical property testing of specimens made using the NH₄F plus Cr powder process exhibited equivalent or higher properties in tensile, stress rupture, and low cycle fatigue compared to the CrF₃ process. These data points have been added to the curves shown in Figures 22-24.

The process incorporating use of fluoride ion cleaning with the NH₄F plus chromium powder as the active fluoride ion source was followed for the 40 piece pilot lot with a typical box load pictured in Figure 33.

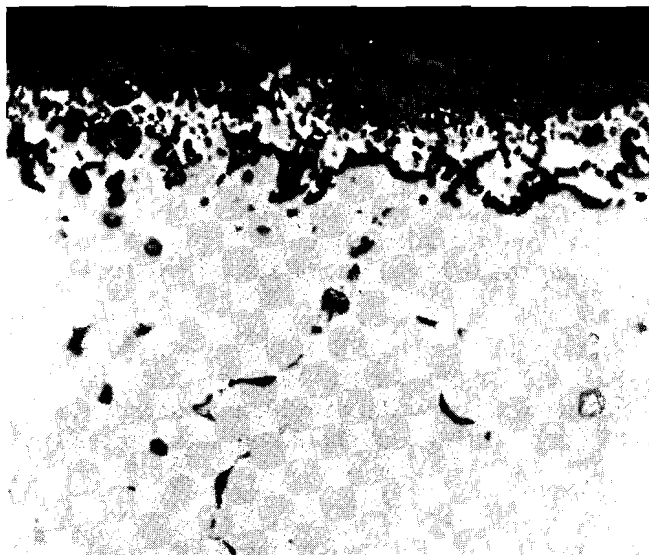
Additional care was exercised to maintain a common ratio between box size, active fluoride ion availability, and surface cleaning area as measured by number of parts cleaned per run. These approximate ratios were held throughout the pilot line run depending on number of parts processed according to the following relationships:

<u>Box Size (cu in)</u>	<u>NH₄F (gms)</u>	<u>Cr</u>	<u>No. Parts</u>
144	130	60	1
576	260	120	4
1513	1520	720	14
1785	1793	850	21



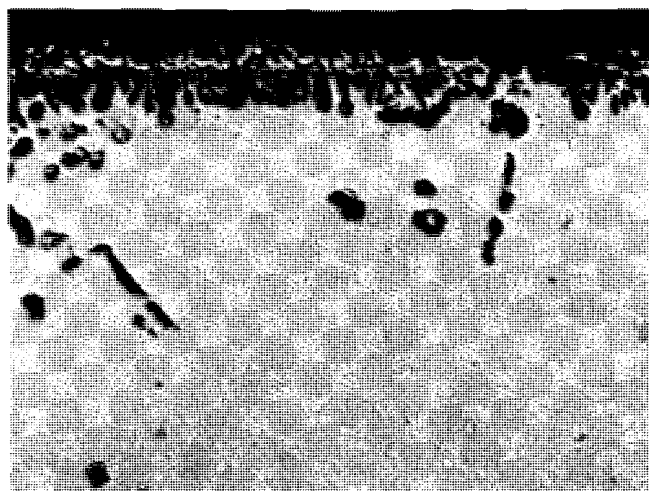
Stage 2 Vane - CODEP stripped
and oxidized at 2050°F/23 hrs.

500X



Stage 2 Vane - CODEP stripped,
F-cleaned w/CrF₃, and oxidized
at 2050°F/23 hrs.

500X



Stage 2 Vane - CODEP stripped,
F-cleaned w/CrF₃, vacuum cleaned
and oxidized at 2050°F/23 hrs.

500X

Figure 29. Oxidation Characteristics of Rene' 80

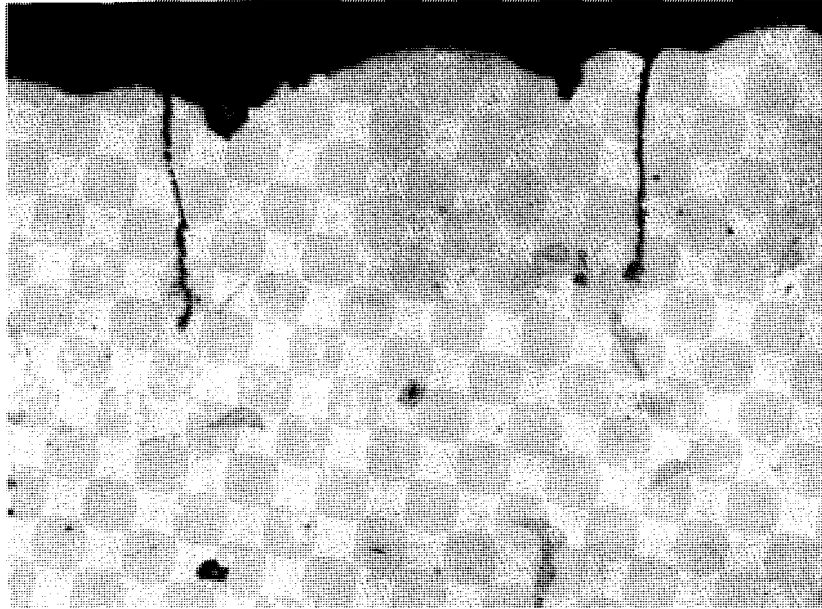
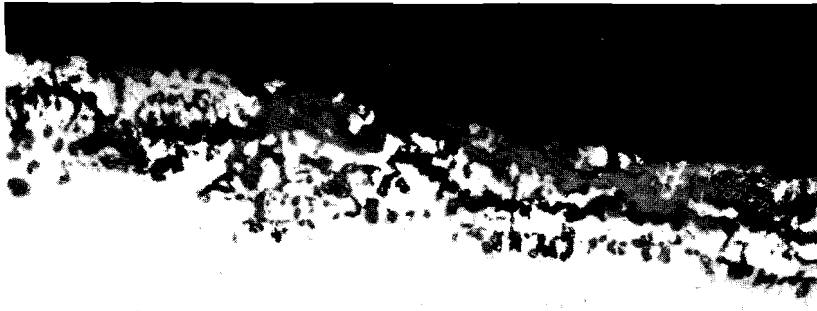
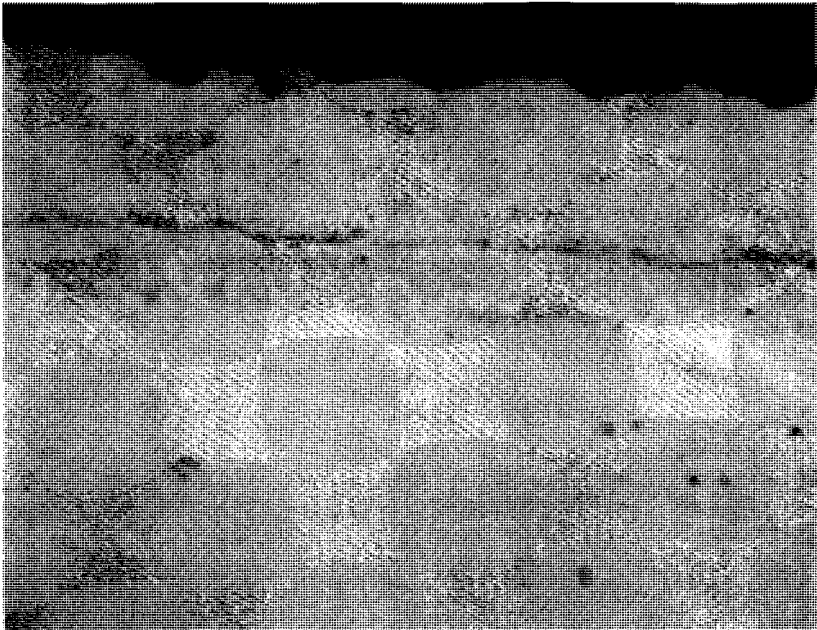


Figure 30. Fluoride Ion Cleaned Vane with .001" Chem Milled from Surface, Codep Coated, and Oxidized at 2050°F/23 Hrs 500x

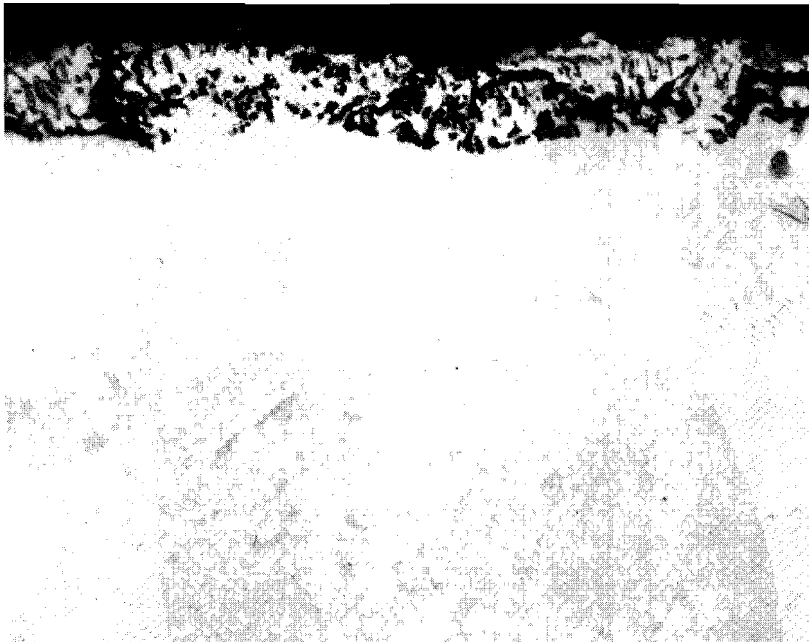


Stage 2 vane CODEP stripped,
F-cleaned w/ NH_4F + Cr, vacuum
cleaned, and oxidized at
2050°F/23 hrs.

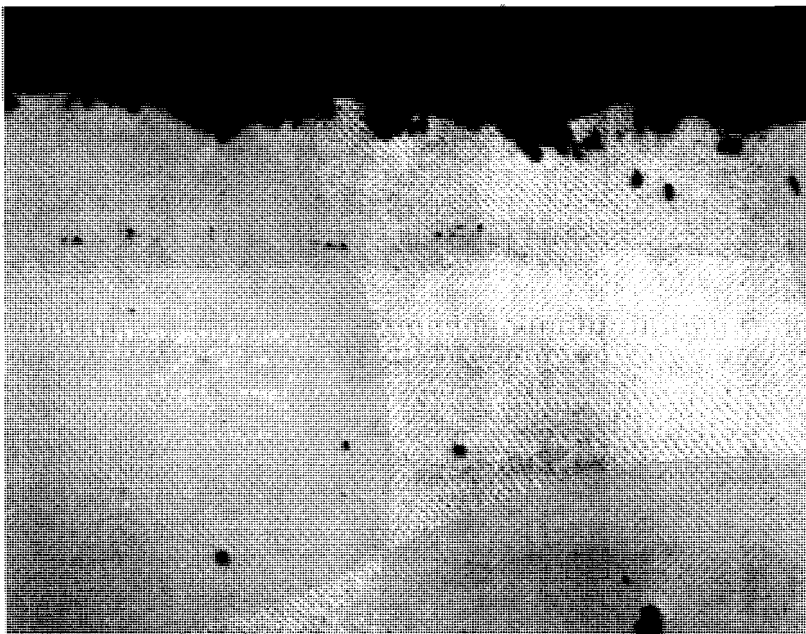


Stage 2 vane CODEP stripped,
F-cleaned w/ NH_4F + Cr, vacuum
cleaned, CODEP coated, and
oxidized at 2050°F/23 hrs.

Figure 31. Stage 2 HPT Vane Fluoride Ion Cleaned and Oxidized 500x



Stage 2 vane CODEP stripped,
F-cleaned w/ NH_4F + Cr, grit
blasted, vacuum cleaned, and
oxidized at $2050^\circ\text{F}/23$ hrs.



Stage 2 vane CODEP stripped,
F-cleaned w/ NH_4F + Cr, grit
blasted, vacuum cleaned,
CODEP coated, and oxidized
at $2050^\circ\text{F}/23$ hrs.

Figure 32. Stage 2 HPT Vane Fluoride Ion Cleaned, Grit Blasted,
and Oxidized

500x

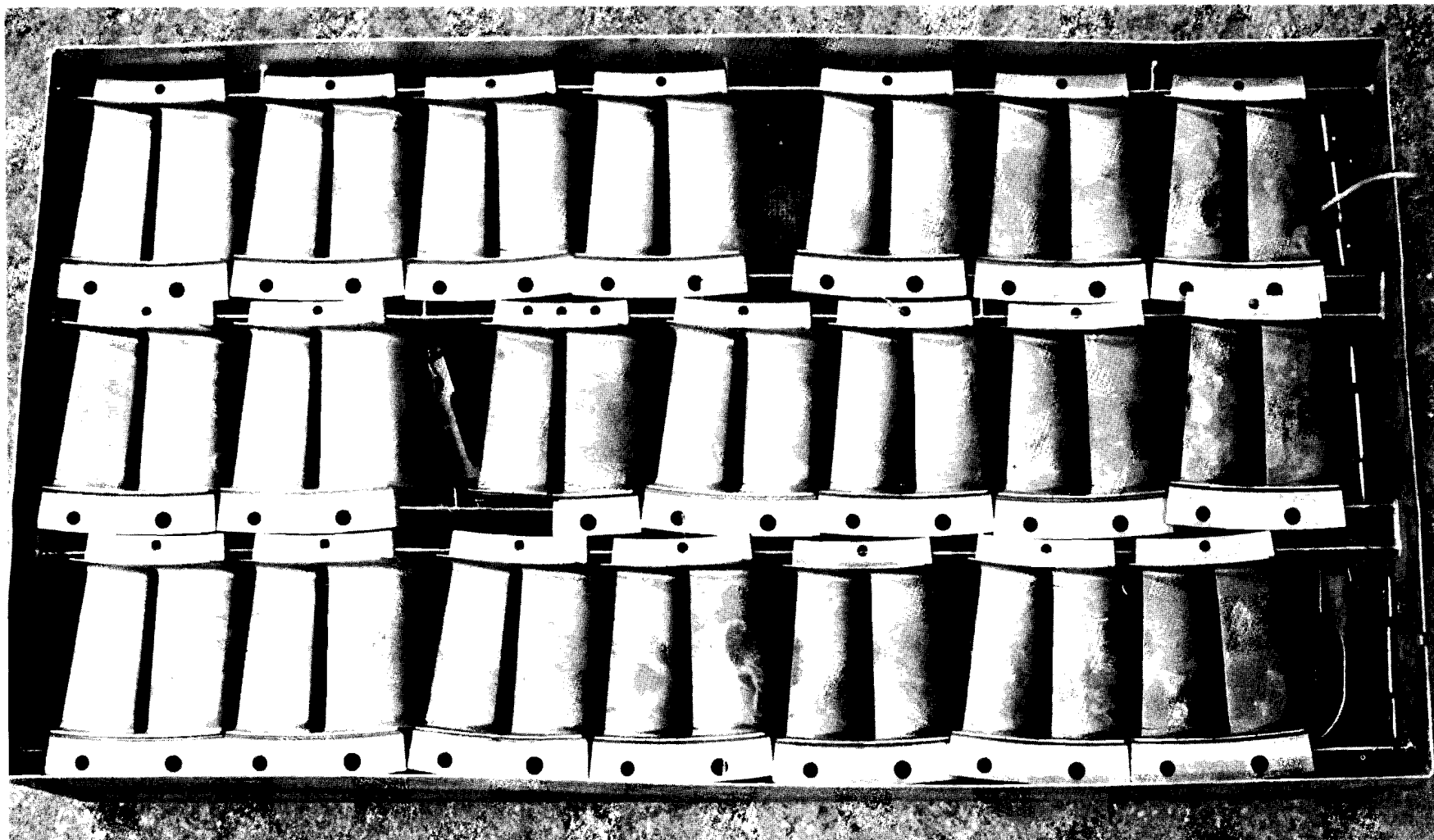


Figure 33. TF39 Stage 2 HPT Vanes Positioned in Container for Fluoride Ion Clean Run

ADH processing of the 40 piece pilot lot was accomplished after the grit blast or dehusk operation and vacuum bright anneal at 2200°F/2 hours. Discrepant areas which were cracked or exhibited worn metal were alloyed with the 50/50 mixture of Rene' 80 and D-15 powder and ADH repaired as illustrated in Figure 34. Metallographic sections taken through scrap vanes processed with the pilot line parts are shown in Figure 35 after the diffusion cycle. The pilot vanes were then blended by grinding and polishing to provide smooth surface contours, finish machined on the bolt hole mounting rails, and Codep coated. Air cooling inserts were installed and the vanes were aged and submitted for final inspection. Figure 36 illustrates the ADH repaired components.

The 40 piece pilot line lot has been completely processed through final inspection with a 100% yield. The ADH repaired stage 2 vanes have been submitted for TF39 engine test and results are expected early in 1979.

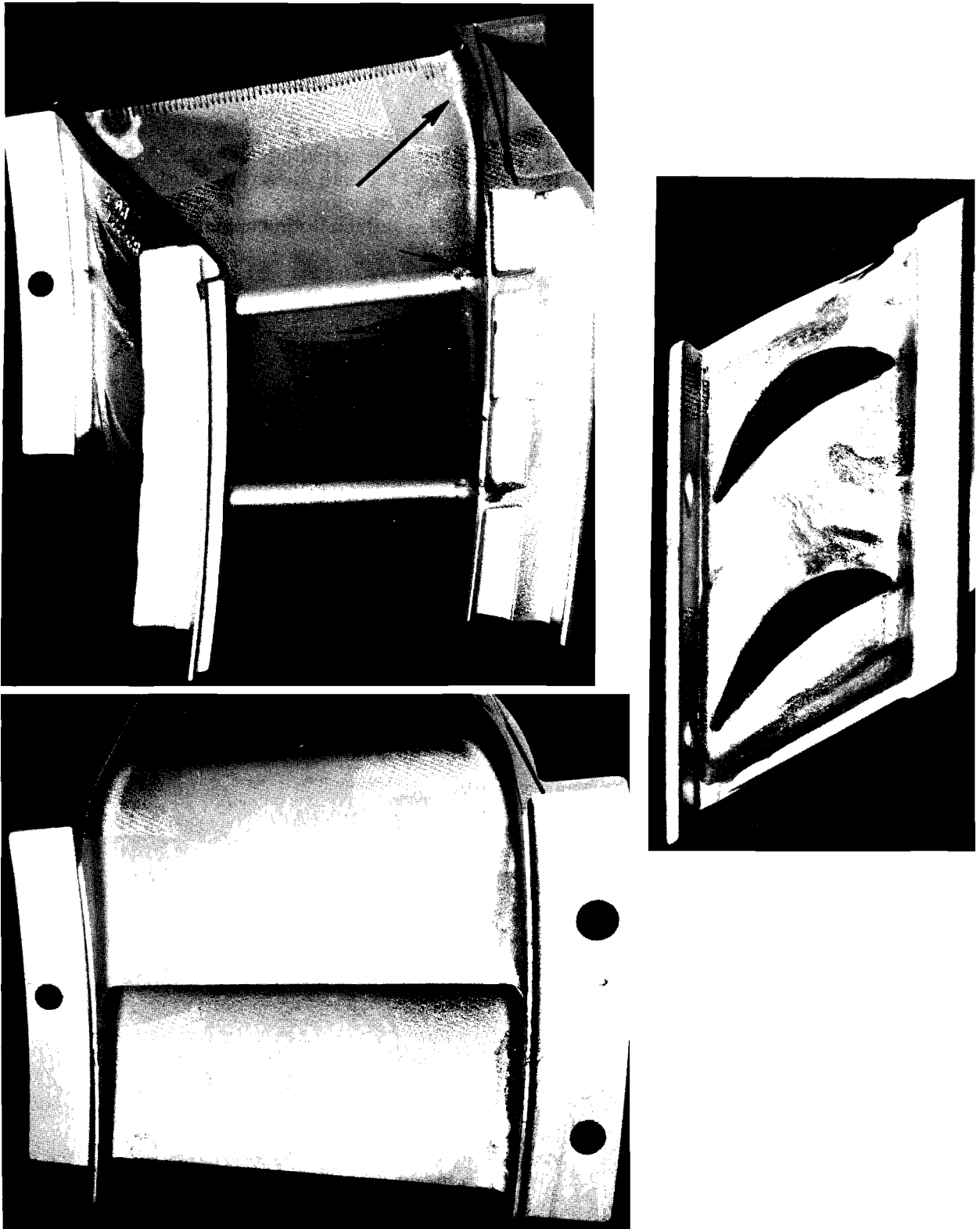
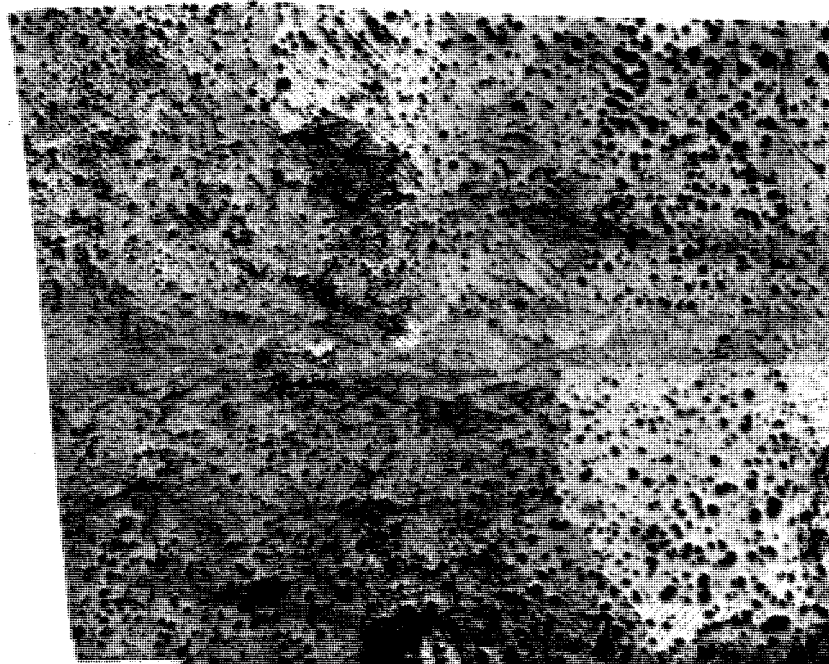
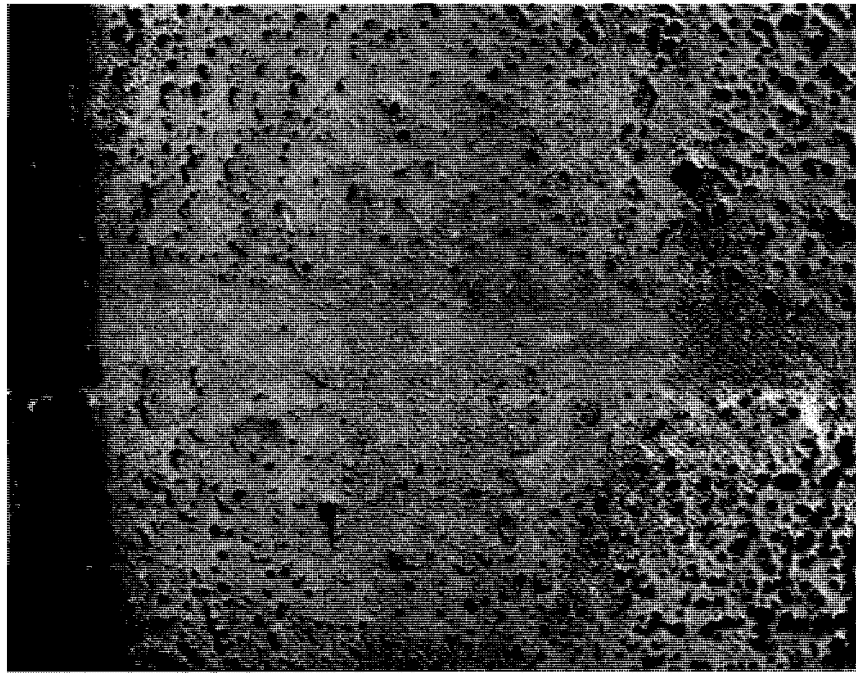


Figure 34. Typical Appearance of F-Cleaned and ADH
Repaired Rene' 80 TF39 Stage 2 HPT Vanes



50X

Figure 35. Photomicrograph of Rene' 80 TF39 High Pressure Vane ADH Repair After Complete Diffusion Cycle

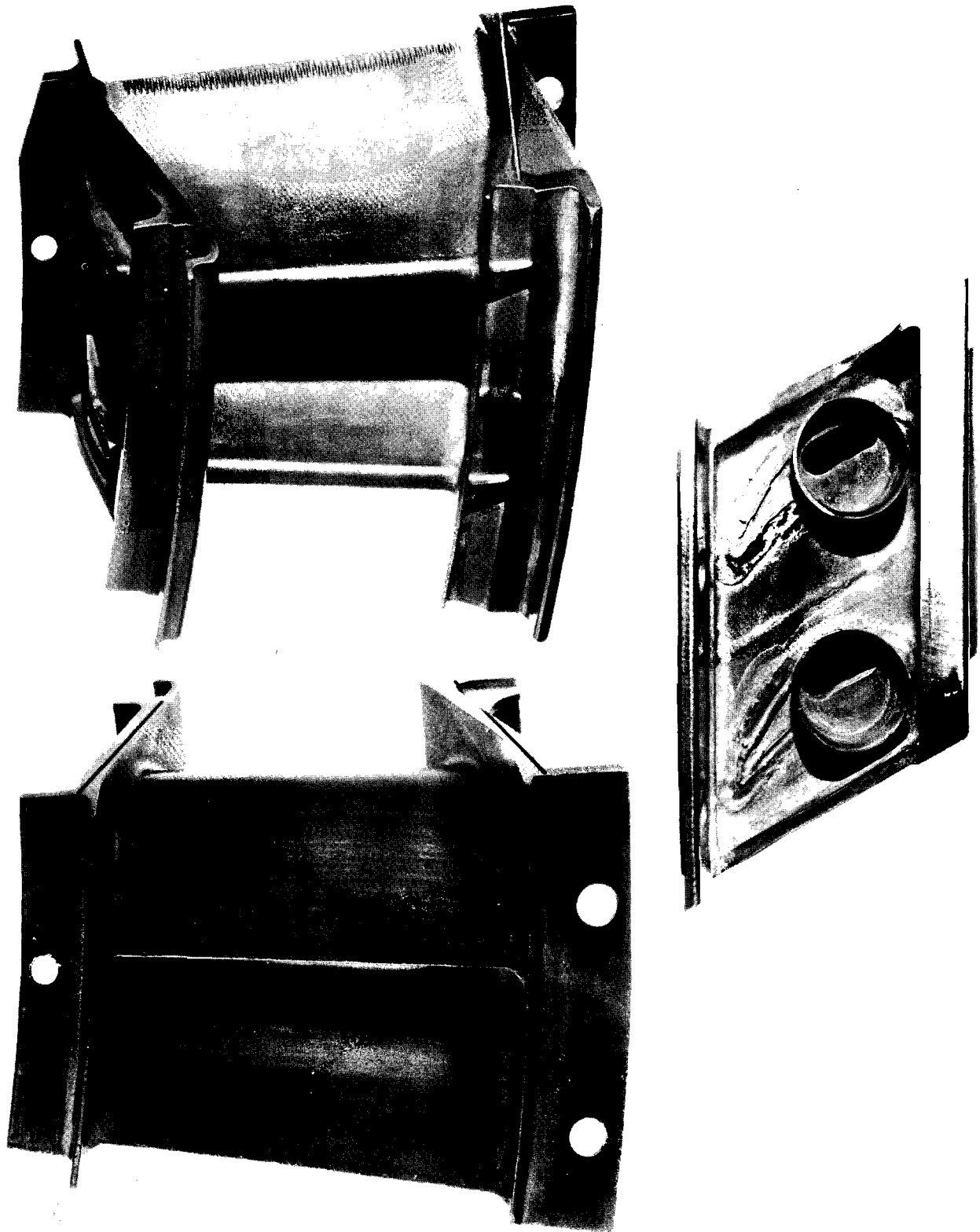


Figure 36. View of Rene' 80 TF39 Stage 2 HPT Vane
After ADH Repair, Codep Coat and Brazing
of Air Cooling Insert

SECTION IV

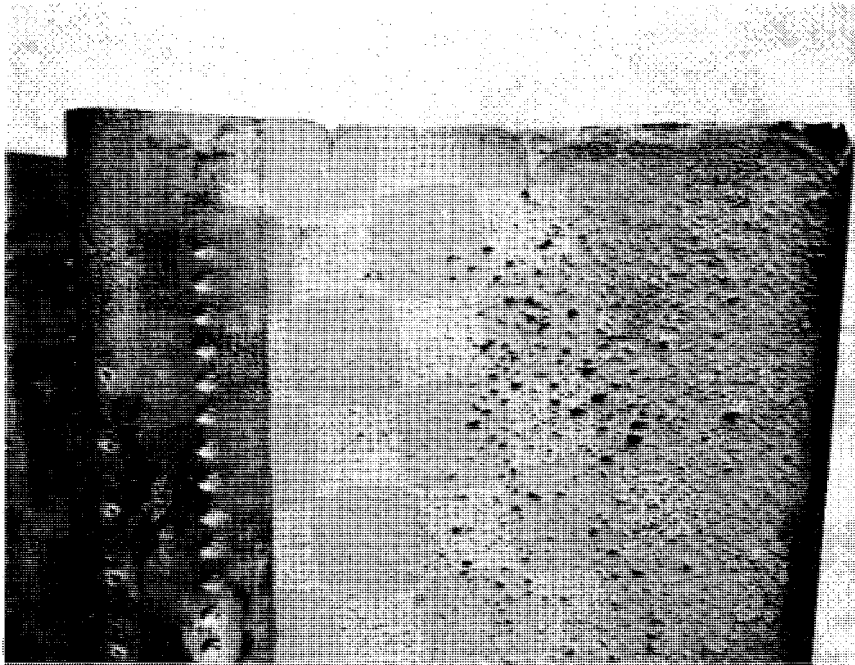
ESTABLISHMENT OF REPAIR PROCESS FOR TURBINE BLADE AIRFOILS

1. TF39 STAGE 1 HPT BLADES

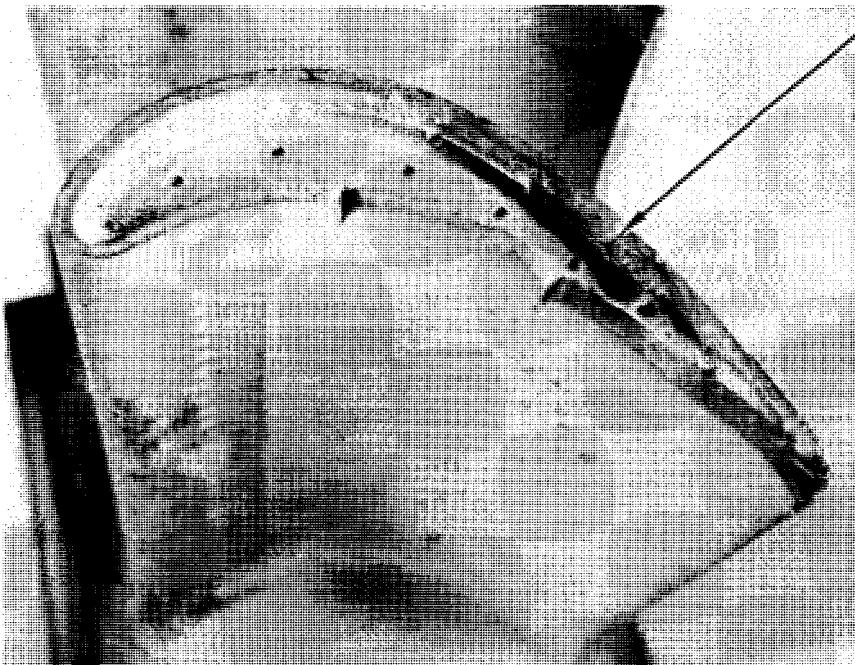
Determination of Repair Procedure and Sequence

The primary goal of this task was to extend the current repairable limits for Rene' 80 blade tip distress. The tip replacement process by mini-bonding was selected as the means by which much serviceable/non-repairable hardware might be salvaged. Excessive tip rub in engine operation generally results in burns and/or cracks resulting at the squealer tip and extending through the tip cap into the airfoil section itself. Figure 37 shows this condition and is illustrative of the potential of a mini-bond repair for replacement of the defective tip and cap. The concept by which the repair was developed is shown in Figure 38. This concept then served as the basis for establishment of the initial repair procedure shown below:

- a. Inspect incoming vane airflow.
- b. Strip Codep coating.
- c. Separate paired blades.
- d. Inspect blades to assess damage and repair needs.
- e. Grind tip for mini-bond repair.
- f. Grit blast clean blade tip area.
- g. Vacuum bright anneal blade to finalize cleaning at 2200°F/2 hours.
- h. Dimensional inspect tip cap height.
- i. Assemble tip cap with presintered D-15 ADB alloy to blade.
- j. Mini-bond tip cap.
- k. Dimensional inspect tip cap height for gap upset and visual inspect for complete bonding.



← 3X SIZE

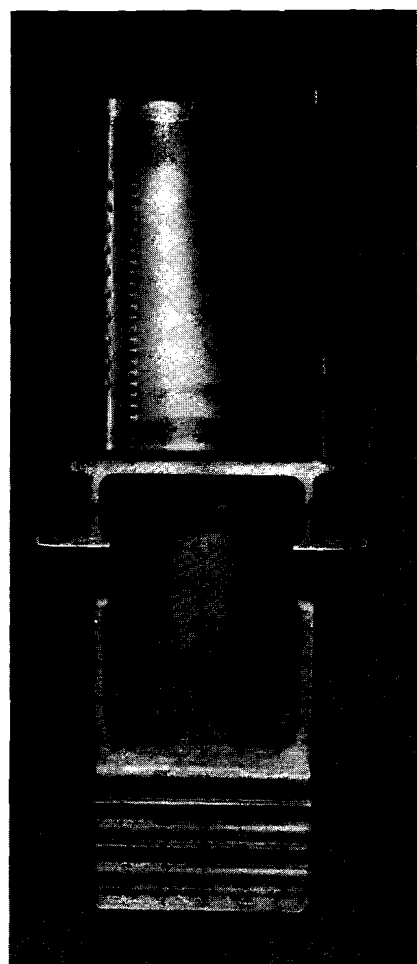


CRACKS THROUGH
TIP CAP

← 3X SIZE

OCCURRENCE
FACTORY \approx 2000 CYCLES

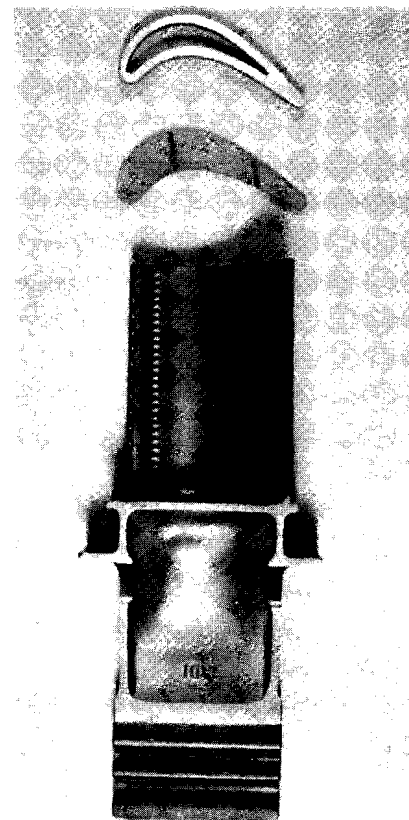
Figure 37. HPTR Stage 1 Blade with Squealer Tip
Cracks Extending Below Tip Cap



MINI-BONDED
SQUEALER TIP

RENE' 80
STAGE 1
HPT BLADE

SQUEALER TIP REPLACEMENT



REPLACEMENT
SQUEALER TIP
MATERIAL

REPLACEMENT
R'80 END CAP

RENE' 80
STAGE 1
HPT BLADE

END CAP AND SQUEALER
TIP REPLACEMENT

Figure 38. Mini-Bond Tip Replacement Concept on TF39/CF6-6
Stage 1 HPT Blade

- l. Dimensional inspect squealer tip height.
- m. Assemble squealer tip, with presintered D-15 ADB alloy, to end cap.
- n. Mini-bond squealer tip.
- o. Dimensional inspect squealer tip height for gap upset and visual inspect for complete bonding.
- p. Bader grind to restore tip geometry.
- q. Grind tip to length.
- r. Dimensional inspect.
- s. Electro-steam open cooling holes as required.
- t. Codep coat airfoils.
- u. Pair braze the blades.
- v. Complete age heat treatment.
- w. Final inspection of all details including dimensional and airflow.

Mini-Bonding Blade Tip Trials

Several problems surfaced in the initial efforts to mini-bond Rene' 80 blade tips to engine run and stripped stage 1 HPT blades. One problem was the formation of excessive oxides at the bond interface which resulted in poor flow and poor joint integrity. Extensive investigation of the vacuum system (leak checks, new diffusion pump, oil, etc), eliminated the vacuum system as the cause for the excessive oxides.

The bonding alloy binder was also eliminated. The cleanliness of the blade itself revealed the source of contamination to be residual Codep on the inside surfaces of the blade which outgassed at mini-bonding temperatures. Subsequently, several blades were re-stripped (with internal cooling passages now exposed), vapor honed, and vacuum cleaned at 2150°F for two hours. Rene' 80 tip caps were then successfully bonded to the blades without oxide formation.

These blades, after metallographic examination, proved acceptable. Twenty more blades were processed, then HS188 squealer tips were subsequently bonded to the Rene' 80 tip cap to complete the blade restoration.

Problems encountered in this process trial, in addition to the oxide problem, were serious temperature control problems. The laboratory mini-bonder used required maximum power output to achieve bonding temperatures. To gain some latitude, the coil configuration was

"fine tuned" to achieve maximum temperature capability. The current concentrator was filed to closely match the blade configuration/current field. With these conditions almost "perfect" blade tip alignment was required to prevent "hot spots" and subsequent over-temperature in a localized area. Furthermore, variation in blade wall thickness also caused localized melting.

These problems resulted in extremely poor yields for the pilot line parts processed in the MPTL mini-bonder. Cap to blade bond yield was 57% while the squealer tip bond was only 21%. Rejects were primarily a result of the temperature control problems and associated with the coil configuration. Because of these problems, work was suspended on the M&PTL mini-bonder and all efforts were devoted to expedite the installation of the Manufacturing Laboratory mini-bonder. A new pilot lot of stage 1 high pressure blades was identified and is in process of being prepared for the tip replacement repair on the MTL mini-bonder.

The MTL mini-bonder should have sufficient power to eliminate the need for close fitting coil to blade configuration and would therefore allow more latitude in temperature control by providing a current field less sensitive to blade wall variations. Process results and component evaluations will be reported in Volume II upon completion of the engine test scheduled early in 1979.

Mechanical Testing of ADB Joints

Test Results

Stress rupture testing of minibonded joints at 2000°F, is shown in Figure 39 and indicates stress rupture values are comparable with the Rene' 80 and HS188 design curves. Although the actual values required for blades cannot be accurately predicted, these values coupled with prior CF6 engine testing of repaired vanes, provide sufficient preliminary data to proceed with TF39 engine testing.

Alloy Application

The initial bonding alloy (D-15) was applied to either the Rene' 80 tip cap or the HS188 squealer tip by "dusting" the braze alloy powder onto the bonding surface which had been acrylic sprayed. This alloy was then sintered to the component at 2000°F for thirty minutes in vacuum. Then bonding was accomplished in the MPTL mini-bonder. The final blades which are fabricated will utilize "Boronized" D-15 foil, which was not available at the program initiation.

Also the "super diffusion" heat treat cycle developed for the ADH braze repair program will be incorporated in the final components bonded in this program. This cycle is designed to eliminate any "borides" formed during the normal bonding cycle.

Quality Control Requirements

Evaluation of the fixture shown in Figure 40 used to determine the ADB joint gap on the mini-bonded blade showed that repeatability was not obtainable when a 'standard' blade was subjected to repeated blade height measurements.

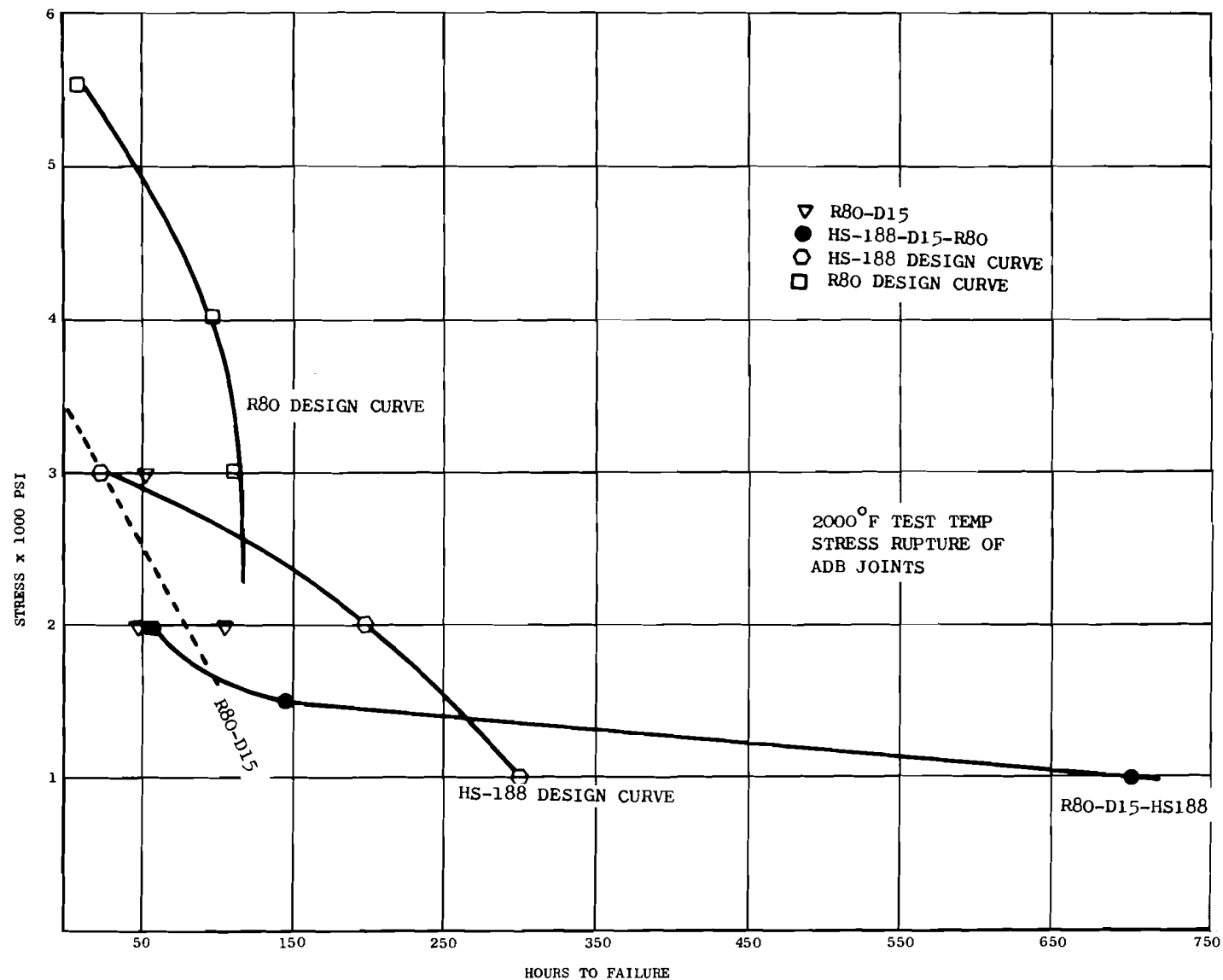


Figure 39. Stress Rupture Test Results of Rene' 80 to Rene' 80 and Rene' 80 to HS-188 ADB Joints at 2000°F

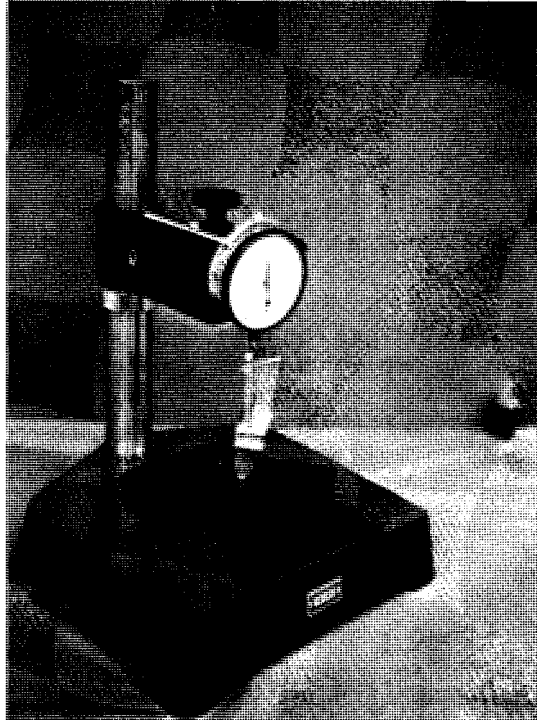


Figure 40. Inspection Fixture Used to Determine
ADB Joint Gap on Mini-Bonded Blade Tips

Modifications of the fixture were made and resulted in a constant position of each blade in the fixture such that repeatable blade height measurements could be made.

Since on the initial run, the bond gap measurements were made using this old fixture configuration, confidence in the accuracy of these measurements is lacking and may account for the high fallout of blades rejected for exceeding the bond gap dimensional limit. To verify the accuracy of the new fixture several blades which had cap to tip bond gaps measured in the fixture using both the old and new configuration were cut to show the cross sections at three measurement points on the joints (see Figure 41) and photomicrographs were made.

Figures 42 and 43 show a typical joint in the as-bonded condition after being run through the diffusion cycle. Bond gap measurements from photomicrographs of the joint are more easily read in the as-bonded condition than after the post diffusion cycle. However, it is useful to see the high quality of the joint after the diffusion cycle has been run. From these photomicrographs the true bond gap can be measured using 100X magnification of these joints. As a result of this comparison it was shown that the new configuration of the fixture accurately measured the true bond gap. Thus, this new fixture configuration shall be used on future blade runs through the pilot line. Unfortunately blades already processed using the original fixture cannot have the bond gap re-measured using this fixture due to the technique involved.

Melting of the blades from the bonding operation and braze voids may be detected during visual and X-ray examinations. Control of braze alloy thickness and density before bonding and more precise temperature control during bonding should result in an improvement in the blade rejection rate due to these defects. Use of braze alloy in sheet form is anticipated to reduce voids as opposed to the present process of dusting alloy onto the parts, and use of more precise temperature measurement devices should result in better temperature control. These control measures should all aid in improving the yield for the mini-bond tip replacement repair process.

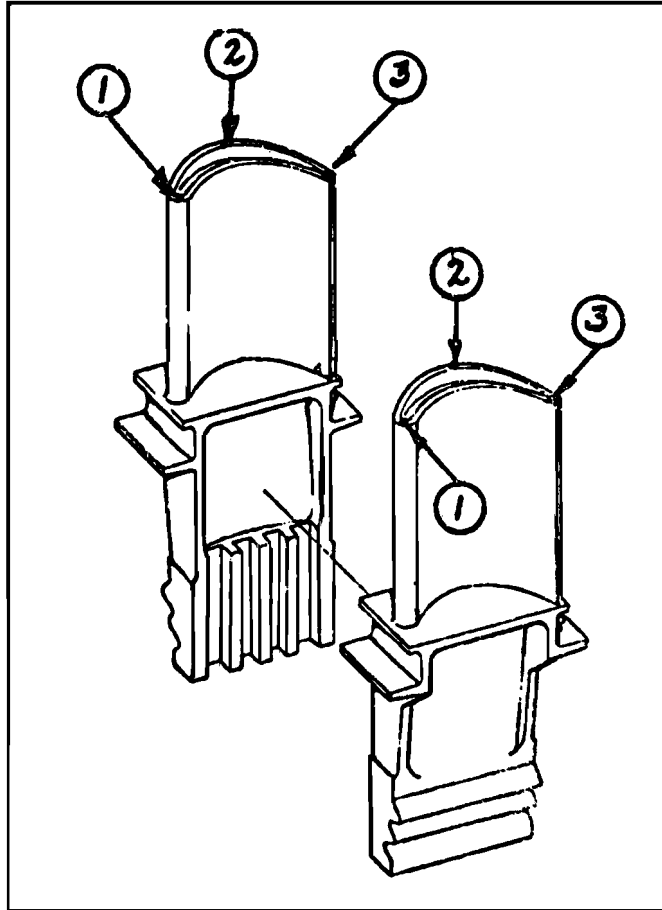


Figure 41. Bond Gap Measurement Locations, Lead and Trail Blades

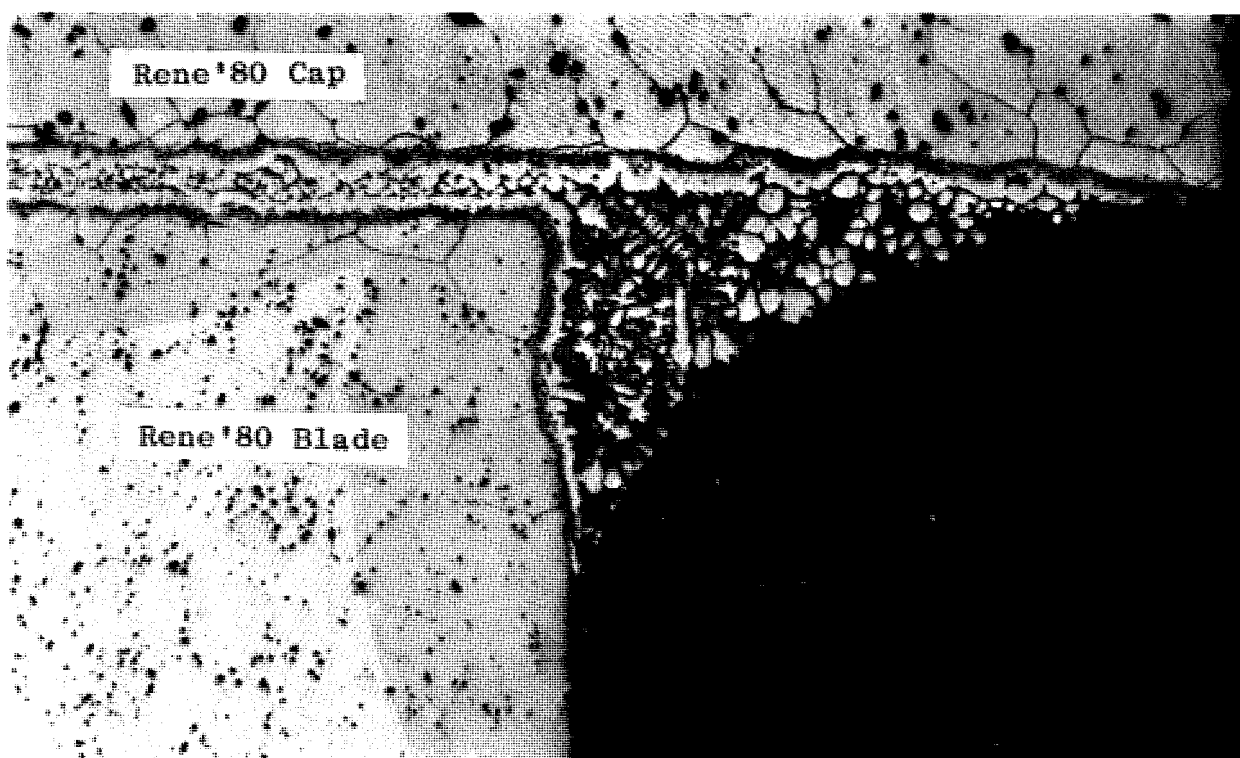


Figure 42. Blade to Cap Joint As-Bonded Prior to a Heat/Diffusion Cycle

100x

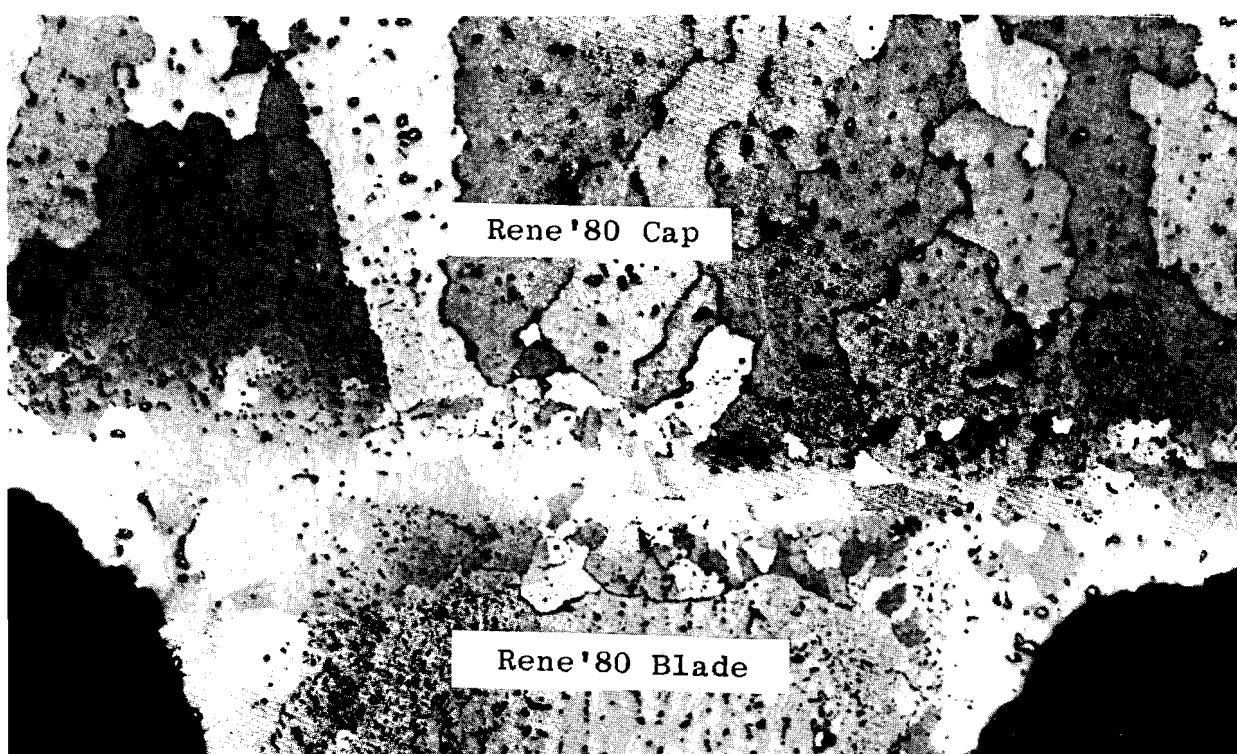


Figure 43. Blade to Cap Joint After a Heat Treat/Diffusion Cycle

100x